UNITED STATES DEPARTMENT OF THE INTERIOR

GEOLOGICAL SURVEY

RESOURCE APPRAISAL OF THE MT. SHASTA WILDERNESS STUDY AREA, SISKIYOU COUNTY, CALIFORNIA

By

Robert L. Christiansen, Frank J. Kleinhampl, Richard J. Blakely

U.S. Geological Survey

Ernest T. Tuchek, Fredrick L. Johnson, and Martin D. Conyac

U.S. Bureau of Mines

Open-file report 77-250

1977

CONTENTS

ILLUSTRATIONS

TABLES

Studies Related to Wilderness

RESOURCE APPRAISAL OF THE MT. SHASTA WILDERNESS STUDY AREA, SISKIYOU COUNTY, CALIFORNIA

By Robert L. Christiansen, Frank J. Kleinhampl, and
Richard J. Blakely, U.S. Geological Survey
and Ernest T. Tuchek, Fredrick L. Johnson,
and Martin D. Conyac, U.S. Bureau of Mines

SUMMARY AND CONCLUSIONS

The only potentially extractable resource of Mt. Shasta may be geothermal energy, but the potential within the Wilderness Study Area is low. Some sulfur and gypsum occur locally around active and extinct fumaroles near the summit but are too small to indicate a resource. Cinder deposits have been mined near the Wilderness Study Area, but almost none are exposed within it. The levels of trace-metal anomalies relative to background values and the amounts of exposed mineralized rock are too small to indicate economic potential.

Mt. Shasta is the largest and one of the highest of Cascade volcanoes. It is near the southern end of the Cascade chain, flanked on the south and west by pre-Tertiary metamorphic and plutonic rocks. A few pre-Tertiary rocks also are exposed near the north base of Mt. Shasta, but the oldest exposures through a large region to the northeast and east are Tertiary volcanic rocks. A complex negative gravity anomaly of nearly 1,200 km^2 extends east and northeast from Mt. Shasta.

Most rocks of Mt. Shasta are pyroxene andesites, emplaced in roughly equal proportions as lava flows and as blocky pyroclastic and debris flows to build a typical stratocone volcano. Hornblende-bearing andesites are less abundant but widely distributed. Small amounts of basalt or basaltic andesite form cinder cones and flows on the flanks of the stratocone, and some dacites occur as volcanic domes, pumice, and sparse lava flows. The stratocone and its subsidiary vents were built on older basalts and andesites from various vents, some of which now lie beneath the stratocone. The summit, at least two older central vents, and a line of flank vents are located along a nearly north-trending slightly arcuate zone parallel to the principal regional faults and to the general strike of pre-Tertiary rocks. Few faults displace the rocks of Mt. Shasta itself.

The Mt. Shasta stratocone grew in at least four major episodes of andesitic cone building. The earliest formed the Sargents Ridge cone, which is older than 100,000 years and now forms the south flank of Mt. Shasta. Dacitic domes and flows were erupted from the summit and flanks late in the Sargents Ridge activity, and some late basalts were erupted from the lower flanks. The next younger major part of the Mt. Shasta stratocone, the Misery Hill cone, is bracketed between the limits of about 100,000 and 12,000 years. A dacitic dome and pumice flows represent the last eruptions from its summit, and a few dacites and basalts occur on the flanks. The third major cone to evolve was Shastina; its central vent lies west of the other three central vents, and the Shastina cone therefore looks more distinctly separate. Late dacitic domes and blocky pyroclastic flows erupted within the summit crater and on the

flank of Shastina. The fourth and youngest part of the stratocone, the Hotlum cone, forms the summit and much of the northeast flank of Mt. Shasta. Most of the Hotlum cone is less than 3,000-4,000 years old. The summit crater is filled by a dacite dome, making the summit of Mt. Shasta the youngest major eruptive unit of the volcano. Its continued cooling sustains two areas of active fumaroles and a hot spring. A lesser eruption may have occurred as recently as 1786.

A detailed new aeromagnetic survey shows a conspicuous band of anomalies along the north-trending line of vents through the summit and connects with an older volcano to the north and with a nearby buried intrusion. These anomalies help delineate the structurally controlled north-trending vent zone. Aeromagnetic anomalies associated with the main part of Mt. Shasta and with Shastina were modeled numerically as a magnetic source bounded by the topographic surface, showing the direction of magnetization to be anomalous; if the bottom of the source is assumed flat and horizontal, the main cone is substantially less magnetic than Shastina. This disparity tentatively is interpreted to reflect a rise in isotherms beneath the Hotlum cone, centered beneath the summit and northeast flank of Mt. Shasta.

The Wilderness Study Area has a low potential for geothermal energy resources. The following indications are favorable: (1) the youngest major volcanic activity was less than 3,000-4,000 years ago, and some eruptive activity may have occurred within the last two centuries. (2) The emplacement of dacites late during each major cone-building phase suggests the possible existence of dacitic magma chambers or solidified but still-cooling shallow intrusive bodies. (3) Small active fumaroles

and a hot spring near the summit indicate high temperatures near the surface; interpretation of aeromagnetic anomalies further suggests somewhat elevated temperatures beneath the summit area. However, the absence of areally significant hydrothermal activity on or near the mountain, the probably high permeability of the hydrologic recharge zone on the stratocone, and the steepness of slopes and instability of terrain in most of the Wilderness Study Area indicate that no major hydrothermal convection system is likely to exist at shallow depth within the stratocone. Any significant potential for future geothermal development is more likely to exist on and near the lower slopes of the volcano, generally outside the study area.

Areas of intense but very localized hydrothermal alteration occur in the central vent areas of each of the four main cones but virtually nowhere else. Very small amounts of sulfur occur locally in these areas, particularly around the fumaroles on the summit dome. Low-level anomalies of some trace elements (lead, zinc, copper, and a few lighter elements), only slightly above background, are associated with some of the altered rocks in the central vent areas. Minor copper minerals are visible on fracture coatings in the center of the Sargents Ridge cone. The low level of the anomalies relative to background and the small amounts of exposed mineralized rock indicate no economic potential.

The Mount Shasta Wilderness Study Area previously has been prospected for mineral deposits, but no commercial grade material was ever found. Courthouse records show that three placer claims were located for platinum. Twenty-four samples taken from the claimed areas contained no significant quantities of economic minerals. Almost no cinder deposits are exposed within the Wilderness Study Area.

INTRODUCTION

Mt. Shasta is the dominant natural feature of Northern California and has been a landmark since the first explorations of the region. The current proposal to establish a Wilderness Area on a major part of the mountain requires an evaluation of its potential for producing valuable mineral or energy resources. Neither Mt. Shasta nor any other Cascade volcano has yet been explored or thoroughly studied for its geothermal potential; in particular no deep drilling has been done. For this reason, more attention has been placed in this study on volcanic stratigraphy, geologic history, and geophysical modelling than commonly is done by the Geological Survey in wilderness studies. The resource appraisal presented here consists of a geologic, geophysical, and geochemical study by the Geological Survey and a study of existing mineral claims by the Bureau of Mines.

Mt. Shasta is a volcano near the southern end of the Cascade volcanic chain of the Pacific Northwest (Fig. 1). Rising to an altitude of 14,162 feet (4,319 m), Mt. Shasta is the second highest (to Mt. Rainier) of the Cascade volcanoes and is the largest of all in volume; Williams (1932, 1934) estimated its volume as 335 km^3.

Fig. 1.--near here

The Mountain is encircled by roads, including Interstate Highway 5 on the west, U.S. Highway 97 on the north, California State Highway 89 on the south, and the unpaved Military Pass Road on the east (Fig. 2). A paved highway to the Mt. Shasta Ski Bowl climbs to an altitude of about 8,000 feet (2,440 m) on the south side of the mountain (Fig. 3), and numerous unpaved timber access roads, many of them unmaintained, give access to the lower parts of the mountain on all sides. The

Fig. 2.--near here

Fig. 3.--near here

Wilderness Study Area occupies mainly the upper slopes of the mountain near and above timberline, which in this region is generally about 9,500 feet (2,900 m). On the northwest side of Mt. Shasta, the Wilderness Study Area extends to near the level of the Southern Pacific Railroad right-of-way at an altitude of about 5,000 feet (1,500 m).

Previous Studies

The geology of Mt. Shasta was first studied comprehensively by Williams (1932, 1934), who prepared a small-scale reconnaissance geologic map, characterized petrographically the main eruptive products of the volcano, and recognized a north-south alignment of eruptive vents across the flanks and summit of the volcano. Later petrologic and geochemical studies of some of Mt. Shasta's lavas were made by Smith and Carmichael (1968), Peterman and others (1970), Steinborn (1972), Condie and Swenson (1973), and Anderson (1974). The only previous geophysical data covering Mt. Shasta and its immediate surroundings are gravity surveys (LaFehr, 1965; Chapman and Bishop, 1967; Kim and Blank, 1972). Recently, detailed studies have been started of the youngest deposits of the volcano, aimed at an evaluation of the volcanic hazards of Mt. Shasta (Crandell, 1973; Miller and Crandell, 1975).

Present Study

Field work was done during three and a half months in the summer of 1975. It included: (1) preparing a new geologic map of the Wilderness Study Area (Fig. 3) and its surroundings (Fig. 2) at a scale of 1:62,500; (2) a new aeromagnetic survey (Figs. 9 & 10); (3) sampling some of the lavas for additional petrographic and chemical analyses (table 2); (4) collecting samples of soils, stream sediments, and altered bedrock for

geochemical characterization of any possible anomalies that might be related to metallic mineral deposits (Fig. 16); and (5) field examination of mining claims (Fig. 23) in and near the Study Area.

Responsibility for preparation of the report has been divided among the authors. Christiansen wrote the introduction, the section on geology, the section on geothermal energy potential, and is responsible for overall coordination and for preparation of the summary and conclusions. Blakely wrote the section on aeromagnetic data and interpretation, Kleinhampl wrote the evaluation of potential for mineral deposits, and Tuchek, Johnson and Conyac wrote the economic mineral appraisal. All authors have helped revise the entire report for internal consistency and accuracy.

Acknowledgments

We acknowledge the helpful cooperation of the U.S. Forest Service, especially District Rangers Ronald Anderson and Dale Trail, in facilitating field work and in accomodating some unavoidable delays in completing the report. The main conclusions of the study reflect the enthusiastic cooperation of C. D. Miller of the Geological Survey, both in the field and in data interpretation. Miller's studies of Mt. Shasta for evaluation of volcanic hazards, done simultaneously and in coordination with ours, have been an essential part of the study of volcanism at Mt. Shasta, reported here. Gerald K. Van Kooten ably assisted in the field work. We thank Arthur Conradi for preparation of the topographic data for aeromagnetic interpretation and Donald Plouff for helpful discussions of the aeromagnetic modeling experiments.

GEOLOGY

Geologic and Geophysical Setting

Mt. Shasta lies near the southern end of the Cascade chain. Of the major cascade volcanoes only Lassen Peak is farther south, and it is offset from the continuous linear belt in which the other major volcanoes of the chain occur (Fig. 1). Mt. Shasta, at the end of this continuous belt, is adjacent to a mountainous terrane of Paleozoic and Mesozoic plutonic and low-grade metamorphic rocks, the Klamath Mountains province, south and west of the volcano. A few exposures of these pre-Tertiary rocks also are present just north of Mt. Shasta, but eastward toward the Medicine Lake Volcano and far beyond, the only exposed bedrock consists of the products of Cenozoic volcanism. A sharp gravity gradient (Fig. 4) marks the overlap between the Klamath Mountains province and Mt. Shasta and its bordering volcanic terrane. The volcanic terrane is marked in the Shasta region by a complex relative gravity low that extends over an area of nearly 1,200 km^2, well beyond Mt. Shasta itself, to include the area northeast and east as far as the Medicine Lake volcano although the latter is marked by a smaller positive gravity anomaly within the larger gravity low. The significance of this large negative gravity anomaly is uncertain, but it may relate to the configuration of the plutonic-magmatic underpinning of this part of the Cascades (for example, see Heiken, 1976). Whether this larger gravity feature reflects an active zone of magmatism within the crust is conjectural, but there is ample geologic evidence of very young volcanism within the zone that is marked by this gravity feature. A conspicuous positive aeromagnetic anomaly is associated with the mountain (Figs. 9 & 10).

Fig. 4.--
near here

Volcanism of Mt. Shasta

Mt. Shasta represents a complex volcanic history, more varied than the massive volcanic stratocone might seem to imply (Christiansen and Miller, 1976). At least four distinct episodes of cone building are clear. Each of these episodes appears to reflect a relatively brief time (less than a few thousand years) of rapid eruption of pyroxene-andesite lavas and pyroclastic breccias from a single central vent, followed by a more protracted period of continued pyroxene-andesitic to more silicic volcanism from the summit and from flank vents. Generally, the longer periods of time between the principal cone-building episodes were dominated by erosion of the stratovolcano.

Rocks and types of volcanic units.--By far the greatest proportion of Mt. Shasta's volcanic rocks are pyroxene andesites. Typically both hypersthene and augite are present as phenocrysts although one or the other may be relatively sparse or even lacking in some rocks. In most of the pyroxene andesites, plagioclase is also a conspicuous and abundant phenocryst mineral, but in a few it is absent or (especially on the lavas of Shastina) present only as very small (1/2 - 1 mm) phenocrysts. Silica contents of the andesitic generally are between about 60 and 63 percent (table 2). A variety of types of inclusions is present in these pyroxene andesites, but the most abundant are fine- to medium-grained mafic dioritic inclusions that consist of plagioclase and hypersthene (± augite). Partial melting effects are texturally evident in some of these inclusions. Other common inclusions include a variety of metasedimentary and plutonic rock types. Commonly the pyroxene andesite flows succeed one another with little or no evidence of erosion.

During the later stages of most of Mt. Shasta's major cone-building episodes, eruption of pyroxene andesites from the central vent alternated with eruption of hornblende-bearing andesites. The latter generally are similar in appearance to the pyroxene andesites. Hornblende commonly occurs as rather sparse phenocrysts along with the two types of pyroxene, but in some units hornblende becomes the dominant mafic phenocryst mineral and augite or both augite and hypersthene phenocrysts may be absent. The hornblende phenocrysts commonly are hollow and have cores of plagioclase; in somewhat oxidized lavas, the phenocrysts generally are oxyhornblende. Typically these rocks have fewer inclusions than many of the pyroxene andesites. Numerous local unconformities give ample evidence of erosion on the cone during the times of eruption of the hornblende andesites.

The andesites occur in similar proportions both as lava flows and as blocky diamictons (very poorly sorted clastic deposits with high proportions of both fine-grained matrix and large blocks--commonly to 10-30 cm, but in many instances to more than 1 m). The diamictons have a variety of origins, and many can be distinguished by features diagnostic of their diverse origins (Crandell, 1971; Crandell and Mullineaux, 1975). Many of these poorly sorted rubbly deposits have angular to subangular clasts and a friable fine-sandy matrix, show common evidence of emplacement at higher-than-ambient temperatures (oxidation rinds or prismatic jointing on blocks, pinkish-colored tops to emplacement units, etc.), and are almost totally unsorted but distinctly tabular in overall form. These features indicate emplacement as pyroclastic flows; texturally most would classify as block-and-ash flows. They generally do

not, however, have glassy shards or pumice as do most ash flows erupted as fragmental ejecta from the vent. These block-and-ash flows generally appear to be hot-avalanche deposits formed by the catastrophic shattering and collapse of materials erupted first as lavas. Other diamictons commonly have at least some rounded to subrounded clasts, have a compact silty or clayey matrix, may or may not show evidence of high-temperature emplacement, and typically have at least a degree of sorting (particularly near their tops or distal margins). These deposits appear to have been emplaced as debris flows of volcanic material; some of them may relate to specific eruptions, especially when the cones were covered by snow and ice, but others may be related to avalanching on the unstable slopes of the volcano during noneruptive times, perhaps related to rapid melting of snow and ice on the slopes of the stratocone while it was still hot, to earthquakes, or to climatically triggered slumping.

Growth of Mt. Shasta by the accumulation of both lava flows and blocky pyroclastic and debris flows have given it the principal features characteristic of the great stratocone volcanoes.

Besides the andesites, which constitute the bulk of the stratocone, there are also more mafic and more silicic volcanic rock types. Basalts and basaltic andesites occur only on the flanks of the stratocone below altitudes of about 7,000 ft (2,100 m). They typically form cinder cones, but some also make extensive blankets of mafic ash. Some occur as lava flows whose sources clearly are the cinder-cone vents. These basalts or basaltic andesites generally have small phenocrysts of plagioclase, olivine, and augite ($\pm$ hypersthene).

The silicic rocks are dacites, generally light in color and with phenocrysts of plagioclase and mafic minerals. The latter are quite varied; some dacites have only hypersthene or only hornblende, but most have both and others also contain augite. Quartz has not been identified as a phenocryst mineral in any of them. The dacites typically form cumulodomes, rather steep-sided accumulations of viscous lava that did not spread very far laterally. However, some of the dacitic vents did erupt continuously long enough to have produced thick lava flows. Some of the dacites were erupted as pumice and form both fallout and pumice-flow deposits. Silica contents of the dacites generally are between about 63 and 66 percent (table 2). Inclusions are common in the dacites, and in some domes they are quite abundant. The inclusions are generally of fine-grained igneous rocks, commonly more mafic than the dacites themselves.

The great stratocone of Mt. Shasta lies among and above several smaller older volcanoes characterized by almost shield-like forms. These volcanoes, including The Whaleback, Ash Creek Butte, and Everitt Hill (fig. 3), are formed of generally dark basalts, basaltic andesites, and pyroxene andesites. In addition to the volcanoes just named, there are similar flows that emerge from beneath the south base of Mt. Shasta and indicate that several of these older volcanoes existed at or near the site of Mt. Shasta before the stratocone was built. It is not clear whether there was a direct genetic connection between these older lavas and the Mt. Shasta pyroxene andesites.

Structural controls.--Williams (1932, 1934) first noted a conspicuous alignment of vents on Mt. Shasta that extends approximately north-south through the summit. Further mapping (Figs. 2 & 3) confirms this nearly linear arrangement of vents although it also defines the existence of many other vents that are not on this trend. The north-trending alignment extends from Signal Butte on the south, northwards through McKenzie Butte, Gray Butte (and perhaps Red Butte if the zone is considered to have a width of about 1 km), Misery Hill, and the Summit (fig. 3); the alignment extends northeastward through North Gate and a series of dacitic domes both southwest and north of it. This zone includes numerous dacitic domes, several basaltic cinder cones, a mixed dacite-olivine andesite vent, and a lava cone of olivine andesite.

Williams (1932, 1934) recognized that this alignment parallels a major regional structural trend in stratified pre-Tertiary rocks south and west of Mt. Shasta and suggested that the alignment was controlled by the strikes of those rocks. The new aeromagnetic survey (see later section) helps delineate this trend and also shows that it extends beyond Mt. Shasta and its own flank vents, making the likelihood of a fracture or fault control parallel to regional trends seem more likely than the strikes of stratified units. Faults parallel to this trend are mapped in pre-Tertiary rocks and in older Cenozoic volcanic rocks southeast of Mt. Shasta although few of them appear to displace the rocks of the stratocone itself.

Williams also suggested that the summit of Shastina and a partly buried vent just to the east (Fig. 2) might lie on an east-west trend that intersects the north-south trend at Mt. Shasta's summit to determine the location of the stratocone. No additional evidence for this east-west alignment has been found, and (as shown in the next section) the main eruptive center of Mt. Shasta has moved four times during the growth of the stratocone; the oldest of these centers lies off the suggested trend. Furthermore, the new mapping shows that there are numerous vents on the north and west flanks of the volcano, suggesting that Shastina and the nearby vent may only be fortuitously aligned with the present summit.

The reconnaissance mapping of Williams (1932, 1934) did not resolve the major age differences between parts of the cone. Local stratigraphic relations suggested to Williams that eruptions along the north-trending alignment of vents were the youngest major events on the main cone of Mt. Shasta. Our mapping indicates that the dacites and basalts of this zone, as well as those on the north and west sides of Mt. Shasta, all represent late stages in their local sequences but that they collectively represent ages spanning most of the stratocone. We conclude that the north-trending zone represents structural control for repeated eruptive events at Mt. Shasta; in parts of the volcanic plumbing system that lay beyond this control (mainly on the north and west sides of the system) vents were distributed more nearly randomly or were controlled by structures of lesser extent.

History of volcanism.--Mt. Shasta evolved over more than 100,000 years. Detailed definition of the cycles in this evolutionary history and their dating have only begun, but some major conclusions are apparent and have important implications for the resource potential of the Wilderness Study Area. The geologic mapping and stratigraphy represented by figures 2 and 3 have been generalized from more detailed work, still only partially completed, both by us and by C. D. Miller of the U.S. Geological Survey.

The Mt. Shasta stratovolcano consists of four or more major overlapping cones; at least the oldest of the four may represent more than one evolutionary cycle in the growth of the stratocone. For descriptive convenience as well as stratigraphic clarity, we have given informal names to the four major component cones so far recognized (Table 1).

Table 1--near here

The oldest cone recognized on Mt. Shasta is centered around upper Mud Creek and is represented prominently by Sargents Ridge, for which it is named (Figs. 2,3,5). A conspicuous feature around upper Mud Creek, upper Sargents Ridge, and the east side of upper Avalanche Gulch is a northward to northwestward dip of lavas and pyroclastic layers. This dip is inward, toward the present summit, and clearly cannot represent flows of lava, hot rubble, or muddy debris from a central vent near the present summit (Fig. 5). Mapping shows that these dips represent only one sector of a radially outward-dipping sequence that was erupted from a central vent just east of upper Sargents Ridge and southwest of the Konwakiton Glacier. Upper Sargents Ridge as far as Thumb Rock (Fig. 5), represents an eroded crater rim concentric to this center. Hornblende andesites are particularly abundant in the upper units of the Sargents Ridge cone, and a dacite dome about 1.5 km south of the Konwakiton

Fig. 5.--near here

Table 2--near here

Glacier (table 2 and fig. 5) was the last lava erupted within its summit crater. Numerous late-stage flank vents erupted dacite and a few erupted basalt or basaltic andesite.

Work by C. D. Miller shows that soils on the lower flanks of the Sargents Ridge cone, beyond the limits of Pleistocene glaciation, are older than the last major glaciation of this region; furthermore, older glacial deposits have been found on these flows at two localities. On the east side of Mud Creek just below Clear Creek, till probably older than the last major glaciation overlies block-and-ash flows of the Sargents Ridge cone and may be overlain by others. On Interstate Highway 5, just north of Black Butte, an old till that must have come from ice on Mt. Shasta overlies volcanic rocks that also probably came from Mt. Shasta. These relations demonstrate that parts or all of the Sargents Ridge cone are older than 100,000 years. This older part of Mt. Shasta may actually represent more than one evolutionary cycle.

The second major cone of Mt. Shasta that we have recognized was centered near the present summit, and part of an old summit dome is preserved on Misery Hill, for which the cone is named (Figs. 2,3,6). Lavas and blocky deposits from this central vent poured across the northward-dipping flows of the Sargents Ridge cone in upper Mud Creek but were prevented by the partially preserved summit rim of the older cone from covering its southern flank. Misery Hill lavas and blocky deposits extend far to the west, north, and east, some of them emerging from beneath younger lavas. The west rim of the Misery Hill summit crater is partly preserved from the head of Avalanch Gulch around the west side of the upper Whitney Glacier (Fig. 6). Late dacitic domes and basaltic cinder cones were erupted on the flanks of this cone. The youngest

Fig. 6.--near here

'units' erupted from the central vent were a dacitic dome (partly preserved on Misery Hill) that filled part of the summit crater, and pumice flows of the Red Banks, which can be mapped over much of the preserved surface of the Misery Hill cone (Fig. 6). Some of these pumice flows and related fallout deposits are recognized farther north on the flanks of the cone, where they emerge from beneath lavas of the two younger cones.

Flows of the Misery Hill cone, even well beyond the limits of glaciation, show soil development comparable to soils formed since the last major glaciation (C. D. Miller, oral communication, 1975-1976); however, the cone was extensively eroded during the last glaciation. Therefore, the cone dates largely from the early part of the last glaciation. Late-stage evolution of the volcano, during which summit and flank eruptions of dacite and basalt occurred infrequently, continued through the last glaciation. The last known deposit of the Misery Hill cone, the pumice of Red Banks, overlies moraines of a minor late Tioga or post-Tioga glacial advance that probably occurred between about 12,000 and 10,000 years ago.

The third major cone of the Mt. Shasta stratovolcano is Shastina (Figs. 2,3,7). Because it was erupted from a central vent at some distance from the other three major cones, Shastina is more obviously distinct than the others. Most of Shastina consists of dark pyroxene-andesite central-vent lava flows with only small phenocrysts of plagioclase (but conspicuous pyroxenes). These flows are quite uniform in appearance and also strongly resemble a lava-flow field erupted from a flank vent on the north side of Shastina at an elevation of 5,900 ft (1,800 m). This flow field (named Lava Park by Williams, 1934) clearly belongs to Shastina although it was not erupted from the central vent.

Fig. 7.-- near here

Many people have regarded the Lava Park flow as very young, estimating its age from the oldest trees growing on it. However, examination of soils on wind-deposited silt within the blocky top of the flow exposed in railroad cuts reveals that it is comparable in age to the other Shastina flows. Williams (1934) also regarded at least one other flow on the northwest side of Shastina, and by implication many of the others as well, as having been erupted from flank vents (see Williams, 1934, p. 236-237; figs. 1,3). Remapping and study of aerial photographs shows clearly that the feature regarded by Williams as a vent is the levee of a flow channel in a lava flow erupted from Shastina's summit. This levee stood high enough to deflect a younger Shastina flow laterally and to form a conspicuous oblique ridge on the northwest flank of the cone (Fig. 7).

The age of the Shastina cone is better known than that of any of the others; cone-building occurred rapidly, in a few thousand years or less. The flows on the north side of Shastina overlie pumice lithologically identical to the pumice of Red Banks (notably including the banding of compositionally distinct types; see Eichelberger, 1975), which is known to be younger than rock-glacier deposits estimated to be between 10,000 and 12,000 years old. Distinctive Holocene soils are found on the lavas and deposits of Shastina (C. D. Miller, oral communication, 1975-1976). The youngest Shastina eruptive events--emplacement of a complex of dacitic domes into the summit crater, lateral explosions and hot avalanches from those domes to produce a fan of block-and-ash flows below Diller Canyon, and the eruption of the Black Butte dome complex and related block-and-ash flows--have been dated by C^{14} techniques and give ages within a range of 9,400 $\pm$ 200 years (Miller and Crandell, 1975; C. D. Miller and R. L. Christiansen, unpublished data).

Fig. 8.--near here

The youngest part of Mt. Shasta is its summit and north and northeast flank, formed entirely by lava flows erupted from a central vent at the present summit (Figs. 2,3,8). The lower parts of most of these flows emerge from beneath the active Bolam, Hotlum, and Wintun Glaciers, but flow levees of several of the largest flows can be traced back up the higher flanks of the cone toward the summit. The youngest major unit erupted from this cone, named the Hotlum cone, is a dome that fills the summit crater; the dome itself contains an irregular linear crater that may reflect explosion or collapse at the vent or disintegration of its core under the attack of acidic fumarolic vapors.

Outcrops of the lower ends of flows from the Hotlum cone overlie lavas and block-and-ash flows of the Misery Hill cone and generally show only weak soil formation. Late Neoglacial moraines, probably less than 1,000-2,000 years old, lie beyond the present termini of the active glaciers on the Hotlum cone but are not flanked by older Neoglacial moraines, 3,000-4,500 years old, although joint work with C. D. Miller shows that their equivalents occur elsewhere on Mt. Shasta even where conditions for ice accumulation are poorer. Therefore, the Hotlum lava flows probably postdate early Neoglacial ice advances of 3,000 to 4,500 years ago; several of the lava flows may be younger than 1,000 years. Preliminary C^{14} dating of volcanic events probably related to the Hotlum cone indicates that some of its eruptions occurred at least as recently as about 200 years ago (C. D. Miller and R. L. Christiansen, unpublished data). The summit dome is the youngest major unit of Mt. Shasta and still has active fumaroles and a small acid hot spring. Fumarole temperatures at 10 separate small vents were measured in July, 1975 at 84°C, probably

boiling temperature for these acid waters at the altitude of 4,270 m, thus indicating that the summit dome probably is still cooling. It is possible that an eruption of Mt. Shasta was observed from the Pacific Ocean in 1786 although the source of that eruption has not been identified clearly (Finch, 1930).

AEROMAGNETIC DATA AND INTERPRETATION

A detailed aeromagnetic survey of the Mount Shasta region was flown in 1975, by commerical contract. The final compiled data consist of two contour maps; one surrounds the main mountain and was flown at an elevation of 2,600 m (Fig. 9), and a second was flown directly over Mount Shasta at an elevation of 4,400 m (Fig. 10). For both surveys, the flightlines were east-west and spaced approximately 1.6 km apart, with two north-south tie lines. Location of the data was accomplished with aerial photographs taken at intervals of approximately 1.2 km for the low survey and 0.7 km for the high survey.

Fig. 9,10-- near here

To prepare the contour maps of figures 9 and 10, the contractor (1) edited obvious machine errors, (2) identified air photos with known surface features, (3) filtered the data (4) adjusted flightlines to agree with the tie lines, (5) removed the IGRF regional field updated to 1975, and (6) contoured the data with an interpolation algorithm.

Most of the obvious anomalies are associated in a general way with topographic features such as Mount Shasta, Shastina, Rainbow Ridge, Black Butte, and Ash Creek Butte. Other anomalies, such as the one over The Whaleback, do not correlate with topography, and interpretation of these anomalies is not as straightforward.

Analysis of the data is summarized here in two steps. First the major anomalies are described, and second a series of inverse and forward modeling experiments are presented for three of the most prominent anomalies: Mount Shasta (including Shastina), Ash Creek Butte, and The Whaleback. Several principal results, constrained by the simple assumptions of the models, were found: (1) the direction of magnetization of Mount Shasta is anomalous, suggesting either that Shastina is more magnetic

than the main part of the stratocone or that the Curie-temperature isotherm rises beneath the main summit; (2) part of The Whaleback appears to be reversely magnetized, and two rather large sources of magnetism lie buried near its south flank; and (3) the magnetization of Ash Creek Butte is concentrated in the lower part of the mountain and probably extends to substantial depth.

Description of the Aeromagnetic Anomalies

A striking feature of the low-elevation map (Fig. 9) is the north-south trend of short-wavelength anomalies, extending entirely across the map. This trend of anomalies overlies a trend in volcanic centers extending north from near Everitt Hill (anomaly A), including Mount Shasta, and terminating over The Whaleback (anomaly B). The magnetic sources producing this chain of anomalies are very near the surface and probably correspond in a general way to the recent extrusive material around the vents that coincide with this trend. The anomalies over Mount Shasta and The Whaleback are discussed later in more detail.

The shoulder of a large positive anomaly is apparent in the extreme southwest corner of the low-elevation map (Fig. 9, anomaly C). This is probably caused by the edge of the Mesozoic mafic and ultramafic masses that are prevalent west and southwest of the aeromagnetic map area (Strand, 1963). Aeromagnetic profiles from near the Mount Shasta region were discussed by Irwin and Bath (1962), and they also observed a correlation between large anomalies and these mafic and ultramafic bodies.

About 8 km north of this anomaly is a moderately large positive anomaly over Rainbow Ridge (Fig. 9, anomaly D). Using the width of constant gradient as a rough estimate of depth to the source (Peters, 1949), we calculate the source to be near the surface. This was unsus-

pected because outcrops at Rainbow Ridge are Mississippian marine sedimentary rocks and Mesozoic metavolcanics (Strand, 1963), materials that have relatively low magnetizations. For contrast, compare the anomaly over Rainbow Ridge with the anomaly over Black Butte, about 5 km farther north (Fig. 9, anomaly E). Black Butte is a 9,000 year-old volcanic plug of relatively more magnetic dacite, yet, compared to Rainbow Ridge, the anomaly is small in amplitude. This suggests that more magnetic material, perhaps part of the ultramafic and mafic complex exposed farther west, lies at shallow depth beneath the surface of Rainbow Ridge.

In the northwest quadrant of the low-elevation map (Fig. 9, anomaly F) is a broad, low-amplitude, negative anomaly. The southeastern corner of this anomaly also appears on the high-elevation map (Fig. 10). The -600-gamma contour of this anomaly in figure 9 traces the field of andesitic flows on the northwest side of Shastina. The negative sense of the anomaly suggests that the flows could be reversely magnetized. To investigate this possibility, a detailed study was conducted to determine their paleomagnetic polarities. Forty-nine oriented cores were collected from eight separate flow units, cleaned by alternating-field demagnetization, and measured with a spinner magnetometer. The average direction of magnetization of all 49 samples has an inclination of 49.9° and a declination of 5.7°, with a 95% cone-of-confidence radius of 4.2°. While this direction is not aligned precisely with either the geocentric dipole or the present earth's field, it does not deviate sufficiently to produce the observed negative anomaly, and other explanations must be considered. For example, a thick sequence of material with relatively low magnetization, such as pyroclastic deposits, may underlie this part

of Shastina to cause the negative anomaly. A second possibility is that the anomaly is an edge effect produced by highly magnetic rocks of a buried mafic and ultramafic complex that is exposed just to the southwest. A. Griscom (oral commun., 1976) has shown by modeling experiments with aeromagnetic data over this mafic and ultramafic sequence that the negative anomaly can be explained by postulating that the ultramafic rocks dip at a low angle beneath the flank of Mount Shasta.

Modeling Experiments

Three of the most prominent anomalies of the survey area were examined in detail by modeling experiments. The source of each of the anomalies was approximated by a body with the topographic surface as its upper boundary and with a flat lower surface. As a first assumption, the magnetization of the source was assumed to be uniform. Then a "best" magnetization vector was calculated using a least-squares inversion from the observed total-field anomaly. Although this is basically the procedure commonly used to successfully model anomalies over seamounts (e.g. Vacquier and Uyeda, 1967; Harrison et al., 1975), any geologist would question the assumption of uniform magnetization of volcanoes in the Mount Shasta area. Consequently, a second step was to examine the residual anomaly, the difference between the observed anomaly and the anomaly calculated from the best single magnetization; the residual represents the errors due to the simple assumptions of shape and uniform magnetization. The residual anomalies either were modeled in forward calculations (i.e., by assuming various shapes and magnetizations, calculating new anomalies, and comparing the computed anomalies visually and statistically to the observed anomaly) or they were interpreted in terms of the geology.

The computer program used for both the inverse and forward modeling was developed by Donald Plouff (1975, 1976) and is a sophisticated version of the method described by Talwani (1965). The program requires that the topographic relief be approximated by a series of horizontal layers, each with vertical sides and polygonal edges. Several statistical parameters are calculated to indicate the precision of the fit. One of these is the "coefficient of multiple correlation", which is unity if the calculated and observed field are in precise agreement and zero if there is no agreement. (See Plouff, 1975, for a mathematical discussion of this parameter.) A normalized standard deviation (S) is also computed to measure the difference between the observed and calculated anomalies. Let the anomaly at point i be h_i and the calculated anomaly at the same point be h_i'. Then

$$S^2 = \frac{\sum_{i=1}^{N} (h_i - h_i')^2}{\sum_{i=1}^{N} (h_i)^2}$$

where N is the total number of field points. S will be zero for perfect agreement between calculated and observed anomalies. This parameter is the reciprocal of the "goodness ratio" described by Vacquier and Uyeda (1967).

The length of the best-fit magnetization vector represents the bulk magnetization of the body. Care should be used in attaching physical significance to this number, however, because it is very sensitive to the assumed size of the body. For example, doubling the three dimensions of the source decreases the magnetization by approximately a factor of eight, depending somewhat on the height of the survey above the source.

Fig. 11.--near here

Mt. Shasta:--Figure 11 shows the digitized approximation to the topography of Mount Shasta. Although as many as 23 layers were used for the modeling, figure 3 shows only the top 15. For reference, the layers are numbered from top to bottom; layers 1 through 7 define the main peak of Mount Shasta, layers 8 through 10 define the peak of Shastina, and layers 11 through 15 are lower on the mountain.

Table 3--near here

Table 3 summarizes the various attempts to calculate the magnetization using inverse modeling. It is clear from table 3 that a source composed of all 23 layers is not a satisfactory model. By successively deleting layers from the top and bottom, the optimum model was found to be layers 1 through 15, with a multiple correlation coefficient of 0.93 and a normalized standard deviation of 0.37. Figure 12 shows the residual anomaly remaining after subtracting the anomaly due to all 15 layers.

Fig. 12.--near here

There are two very pertinent results from this experiment. First, because the entire mountain is normally magnetized and therefore less than 0.7 million years in age, we expect the direction of the remnant component of magnetization to be very close to the direction of a field produced by a geocentric dipole (inclination = 61°, declination = 0°). Induced components of magnetization will parallel the regional field of the area (inclination = 65°, declination = 19°). But the direction determined by least squares differs substantially from any combination of these directions (inclination = 45.0°, declination = 51.3°).

This discrepancy can be explained in at least three ways. The first is by tectonic rotation of the mountain, which we discount on geologic grounds. The second is by an error in the location of the

anomaly relative to the topography. We have reexamined the aerial photographs and the contractor's analog data and find no evidence of this type of error. The third and most likely explanation is that either the assumption of uniform magnetization or the assumed shape of the source is too simple. For example, if the distribution of magnetization is such that the anomaly is displaced relative to an anomaly produced by uniform magnetization, the naive assumption of uniform magnetization calculates a spurious direction.

The second pertinent observation appears in the residual map of Figure 12. The low residual anomaly over the main peak of Mount Shasta and the high residual over Shastina suggest that Shastina could be substantially more magnetic than the rest of Mount Shasta. To investigate that possibility, various forward models were tried by varying the magnetization of the layers. With J = 0.0152 emu/cc for Shastina (layers 8 through 10) and J = 0.00152 emu/cc for the remainder of the mountain, the fit improves considerably and has a standard deviation of 0.32. Within the constraints of this simple model, Shastina is more magnetic than the remainder of the mountain by a factor of ten. It is of interest to note that to obtain this excellent fit it was necessary to maintain the anomalous direction determined by least squares. For comparison to the model result, magnetic analyses of 12 rock samples from various locations on the mountain are presented in table 4. The average value of susceptibility for all rocks is 0.075×10^{-3}, and there is no statistical difference between the susceptibility of Shastina samples (0.071×10^{-3}) and other Mount Shasta samples (0.079×10^{-3}). For remanent magnetization, the average of all rocks (excluding those suspected on the basis of demagnetization experiments to have been

Table 4.-- near here

struck by lightning) is (0.201×10^{-3}) emu/cc, and there is no statistical difference between Shastina samples (0.220×10^{-3} emu/cc) and other Mount Shasta samples (0.186×10^{-3} emu/cc).

The contradictory results of the modeling experiments and the magnetic analysis suggest something fundamentally different about Shastina and the main peak of Mount Shasta (Blakely and Christiansen, 1976). Perhaps the interior of Mount Shasta beneath the summit has a larger fraction of pyroclastics than Shastina, thereby reducing its magnetization. A second possibility is that the Curie-point isotherm rises beneath the Hotlum cone, effectively decreasing the size rather than the magnetization of the magnetic source beneath the summit. No heat-flow data exist to prove or disprove this idea, but fumarolic activity near the summit of Mount Shasta is not matched on Shastina. Moreover, the Hotlum volcanic episode, from which the summit dates is at least 4,000-8,000 years younger than the Shastina episode, and magma may still exist at shallow depths beneath the summit of Mount Shasta.

Ash Creek Butte:--The largest anomaly of the entire survey area is located over Ash Creek Butte in the northeastern quadrant of Figure 9 (anomaly H). Ash Creek Butte is a glaciated late Cenozoic basaltic-andesite volcano.

Fig. 13.--near here

Table 5--near here

Fig. 14.--near here

Figure 13 shows the digitized approximation to the topography of Ash Creek Butte, and Table 5 provides the results of inverse models using different combinations of layers. As before, layers are numbered consecutively from top to bottom. The best model (Fig. 14) consists of only the bottom two layers, suggesting that the magnetization of Ash Creek Butte is concentrated near its base; i.e., below an elevation of 1,952 m. This two-layer model provides a correlation coefficient of

0.92 and a standard deviation of only 0.39. Moreover, the residual field shown in figure 14 is very smooth compared to the observed anomaly (fig. 9). This excellent fit is surprising in view of the simplicity of the model.

The intensity of magnetization for this two-layer model, however, is 0.0297 emu/cc which is unreasonably large for common volcanic rocks. This number could be reduced by lowering the bottom of the source to greater depths, thereby increasing its volume, and this would probably not substantially deteriorate the least-squares fit. But in order to reduce the magnetization to a more reasonable value, say 0.01 emu/cc, the bottom of the body must be placed nearly 1.5 km below the base of the butte. We suggest that the substructure of Ash Creek Butte is an intrusive plug; although there is no direct evidence for such a conclusion, it is geologically reasonable.

The Whaleback.--A third set of large anomalies (Fig. 9,, anomaly B), is associated with The Whaleback, a double-peaked volcanic butte composed of Quaternary basalts and andesites. A moderately large positive anomaly lies over the main western peak, but the anomaly over the eastern peak is negative. Geologic reconnaissance suggests that the eastern peak is somewhat older than the western one, and the negative aeromagnetic anomaly suggests that it probably is older than 700,000 years, the time of the latest geomagnetic reversal. The picture is confused, however, by two large anomalies, one negative and the other positive, which lie just to the south of each peak but too far away to be related simply to the topography.

Fig. 15--near here

The topography of The Whaleback was approximated digitally (Fig. 15) and the anomalies were inverted to obtain an optimum magnetization vector. The correlation coefficient for this experiment was only 0.56 and the normalized standard deviation was 0.82. This poor fit implies that the assumption of a uniformly magnetized source confined by the topography is not adequate. As a preliminary interpretation, we suggest that the two northerly anomalies are produced by the two peaks of The Whaleback and that these are of different ages. The sources of the two southerly anomalies are postulated to be at shallow depth below the surface, and perhaps are buried intrusive bodies. The western buried source is reversely magnetized.

Summary

Many of the aeromagnetic anomalies of the Mount Shasta area are due to sources with shapes controlled largely by the topography. The aeromagnetic data suggest however, that there may be buried sources beneath Rainbow Ridge (ultramafic rocks) and south of The Whaleback (buried shallow intrusive bodies). A regional feature of the aeromagnetic map is a nearly linear, north-south trend of anomalies correlated with volcanic centers from near Everitt Hill through Mount Shasta to The Whaleback. Within the Wilderness Study Area, there is no evidence from the aeromagnetic data of any body of igneous rock that might be mineralized.

Modeling experiments using the anomaly over Mount Shasta (including Shastina) show that (a) the average direction of magnetization is anomalous, and (b) the main peak is substantially less magnetic than Shastina. The latter observation is tentatively interpreted as a rise in isotherms under the summit area.

The anomaly over Ash Creek Butte is the largest of the survey area, and model calculations suggest that the source is concentrated at and below the topographic base of the butte. The actual source may be a buried intrusive mass such as a mafic volcanic plug, but it must be substantial in size.

Our inverse results are rather complicated when compared with the more straightforward results from the same technique on seamounts (e.g., Harrison and others, 1975). The difference results partly from our higher density of data (flightlines spaced only 1.6 km apart as compared typically to a few shiptracks) and from the greater proximity of our magnetometer to the source (81 m from the summit of Mount Shasta as compared typically to several hundred meters from seamounts). But at least part of the difference probably arises because land volcanoes are indeed more complex than seamounts. Vacquier and Uyeda (1967) made similar observations when they compared inversion results from nine Pacific seamounts with those from three land volcanoes in Japan. The processes building typical stratovolcanoes and typical seamounts are fundamentally different just as oceanic crust is fundamentally different from continental crust.

RESOURCE POTENTIAL

Geothermal Energy

The only areas of development or active exploration for geothermal resources in the United States are associated either with young silicic volcanic rocks or with regions of exceptionally high heat flow in extensional tectonic zones. Such areas include The Geysers, the Imperial Valley, the Coso Mountains, and Long Valley in California; the region of northern Nevada, southeastern Oregon, and southern Idaho; Roosevelt Hot Springs, Utah; and the Valles caldera, New Mexico. To date, the largest geothermal systems with the highest temperatures in the United States and elsewhere generally have been found to be associated with young silicic volcanic fields (Smith and Shaw, 1975). There has been relatively little active geothermal interest in the andesitic stratovolcanoes of the United States, but regions characterized by such volcanoes are being explored or exploited for geothermal energy in Indonesia, the Phillippines, Japan, Kamchatka, Mexico, Central America, and elsewhere.

None of the Cascade volcanoes has yet been explored or studied in detail for its geothermal potential, and no significant information from drilling exists. In the absence of detailed geophysics and good subsurface data, the only approach to evaluating the potential of a volcano such as Mt. Shasta for possible geothermal resources is to use geologic and regional geophysical data to interpret possible subsurface conditions and to suggest areas for more specific exploration. This is the approach adopted here for Mt. Shasta.

Several geologic and geophysical indications are favorable to the possibility of a geothermal resource associated with Mt. Shasta. First, the revised volcanic history and stratigraphic dating indicate that a major phase of volcanism, the Hotlum episode, is younger than 3,000-4,000 years, and perhaps is only 1,000-2,000 years old. The possibility of an eruption less than 200 years ago has been widely known since the brief note of Finch (1930). These factors, along with the active small hydrothermal features near Mt. Shasta's summit, suggest a viable heat source beneath the summit and northeastern sector. Second, the repeated history of emplacement of dacitic domes and flows at the summits of each of the four successive cones of Mt. Shasta, as well as along the flanks of at least three of them, during their waning stages of activity show that silicic magma has been introduced repeatedly to shallow levels. Since such silicic magmas, emplaced during the late stages of cone building, may represent the products of magmatic differentiation in high-level magma chambers, and since these silicic magmas (regardless of origin) are generally more viscous and may tend to accumulate more readily in crustal magma chambers than the andesites, there is a high probability that such chambers were formed within or just below the volcanic edifice during four separate episodes. At least the youngest of these is likely to still be at solidus temperature, and at least two of the others are less than 100,000 years old and probably are still hot although solidified. Third, the presence of two small active fumarolic areas and an acidic hot spring near the summit clearly indicate high temperatures at shallow levels within the volcano. The favored aero-magnetic interpretation suggests that the main cone of Mt. Shasta is hotter at shallow depths than Shastina, lending credence to the indirect geological evidence of a viable heat source.

Balanced against these favorable indications, additional geological features tend to indicate that any geothermal resource is more likely to be within drilling depth around the flanks of the volcano, outside the Wilderness Study Area, than directly beneath the main cone. First, the very small hydrothermal features near the summit are the only such manifestations at the surface anywhere on the stratocone. Any large hydrothermal convection system at shallow depth within the cone would be expected to have obvious manifestations. Second, Mt. Shasta is a major site of precipitation, mainly as a deep winter snowpack, and is a principal groundwater recharge area of the region. High porosities and permeabilities of both the lava flows and the blocky pyroclastic flows that constitute most of the stratocone are indicated by the intermittent character of most drainages from the mountains. This high permeability and the lack of significant weathering or alteration in most of the cone--which might have created locally impermeable clay-rich zones--suggest that precipitation on the stratocone is largely transmitted with little delay to the groundwater aquifers around it and does not tend to reside long enough in the cone to favor the development of significant hydrothermal convection. Third, the elevation, steepness of slopes, instability of frequently snow-covered slopes, lack of suitable construction sites, and greater necessary depth of drilling to any probable heat sources all make the likelihood of an exploitable geothermal resource directly beneath the main stratocone and the Wilderness Study Area seem remote.

In combination, the foregoing interpretations suggest that a geothermal resource could exist at depths that could be drilled from Mt. Shasta's lower flanks, but in the absence of significant surface hydrothermal features, heat-flow measurements, or pertinent geoelectric studies such a possibility cannot be confirmed. One possibility might be the long-range feasibility of extraction of energy from hot dry rocks in the pre-Tertiary basement beneath the lower flanks of the volcano, especially on the north side, where pre-Tertiary rocks are exposed closest to the youngest part of the stratocone. It is unlikely that any economic geothermal resource would be located beneath the Mt. Shasta Wilderness Study Area.

Mineral Deposits

Regional distribution and general features.--The "forty-niner" era of gold mining and exploration inaugurated by the 1848 discovery of gold at Sutter's Mill, California, along with discoveries on the Trinity River southwest of Mt. Shasta the same year, gave impetus to exploration for metal throughout California (Clark, 1966, p. 181). Shortly thereafter, Mount Shasta and the surrounding region undoubtedly were prospected intensively. It is obvious from the near absence of prospect pits on Mount Shasta that no favorable indications were found.

Mineral deposits nearest to Mount Shasta include base- and precious-metal, asbestos, chromite, iron, manganese, and quicksilver to the west and south in the Klamath Mountains province (Albers, 1966, figs. 4,5). The nearest of these deposits are within 20-25 km of Mount Shasta, and all are in pre-Cenozoic rocks. Two other precious-metal districts about 115 km east of Mount Shasta, the Hayden Hill and Winters districts, are in Tertiary volcanic rocks. Closer by, mining has been confined to numerous industrial mineral deposits, such as perlite, pumicite, obsidian, cinders, and sand and gravel (Chesterman, 1956; Gay, 1966, fig. 2 and p. 97).

Prospect pits and other artificial disturbances common to mineralized regions are very rare in the study area. The only mining operation in the area is a small volcanic-cinder pit at the south edge of sec. 34, T. 41 N., R. 3 W., that has been quarried for the road metal used on some timber access roads. Other cinder pits are located near but outside the study area.

Exposed bedrock on the lower flanks of Mount Shasta within the study area is generally unaltered. Exposed altered areas are mostly in the core areas of the four component cones of the stratovolcano, near the summits of Mount Shasta and Shastina and on the north end of Sargents Ridge and upper Mud Creek. The altered zones examined on Sargents Ridge consist of widespread iron-oxide-stained rocks and local irregular patches of weakly silicified material. Bleached and weakly propylitized rocks extend northeast across Mud Creek. Some of the altered areas represent sites of past thermal-spring or fumarolic activity. Currently, fumaroles near the summit of Mt. Shasta are depositing sulfur; gypsum veins of slightly greater extent occur around the summit areas of Mt. Shasta and Shastina.

Veins are very scarce; most commonly they are fracture-fillings. The prevalent filling material is iron oxide, with lesser chalcedony or vein quartz. None of the veins are large, persistent, or abundant. The largest ones found are near the head of Brewer Creek (at sample locality 75SK-65, fig. 16 lab. no. LDA-096) and consist of quartz-filled fractures only a few meters long and a few centimeters thick. Some discontinuous anastomosing chalcedonic quartz veinlets occur in irregular zones within flows in the same area.

Geochemical Exploration

Methods:--A total of 128 samples, including 48 stream sediments, 53 altered rocks or fracture coatings, 21 unaltered volcanic rocks, and 6 soils, were crushed if necessary and sieved. The minus 80-mesh fraction was analyzed by a semiquantitative 6-step emission spectrographic method. This scan provided initial data on 30 trace elements that are typical of many metalliferous mineral deposits and data on 5 other common elements (iron, magnesium, calcium, titanium and manganese). Analytical data for mineralized samples are given in table 6.

Table 6.--> near here

Obviously mineralized samples, and samples found by the initial spectrographic scan to contain unusually large amounts of some trace metals, were further analyzed by more sensitive methods for antimony, arsenic, copper, gold, mercury and zinc.

All samples were analyzed in laboratories of the U.S. Geological Survey. N. M. Conklin of the Analytical Laboratories Branch performed most of the spectrographic analyses; a remaining seven were analyzed by L. Mai. J. D. Hoffman of the Field Services Section analyzed for mercury using a mercury detector; J. Crock did the atomic absorption-analyses for copper and zinc; G. Riddle and Crock analyzed for arsenic by a graphite-furnace atomic-absorption method; Burrow analyzed for antimony by a rhodamine B method; and Crock, Hafftey, and Haubert obtained fire-assay and atomic-absorption analyses for gold.

The field sampling procedure was to collect stream-sediment samples systematically and to collect altered rocks or fracture coatings wherever they were noted. Twenty-one bedrock samples from nonmineralized localities, including 7 of the more silicic rocks, were selected to represent the main volcanic units for background contents of trace elements

Table 7-- near here

(table 7). Background values were established by empirically evaluating the analyses of the unaltered volcanic rocks and by comparison to the apparently mineralized samples as well as to general backgrounds and averages for similar intermediate and mafic volcanic rocks of other areas (Hawkes and Webb, 1962, Rankama and Sahama, 1950, and Parker, 1967).

Fig. 16.-- near here

Figure 16 indicates the sample density for all types of samples; coverage of the area is fairly uniform. Nonuniform distribution of certain sample types results from the localized absence of collectable materials rather than from a nonuniform distribution of sample localities.

The stream sediments represent integrated samples of the upper parts of the stratocone; however, not all streams heading in the mountain were sampled. Stream-sediment samples were taken at a general spacing of about 400-800 m along the major stream courses, with a range in spacing of 200-2,000 m. Each stream-sediment sample generally is a composite of material selected from along about 3-15 m of stream course. Some samples are from a single site; others are composites from several sites scattered along as much as 400 m of stream bottom. Sediments were taken from the beds of active streams, from terrace deposits adjacent to active streams, or from beds or terraces of dry stream channels. Fine material was taken wherever possible. For each sediment sample, an attempt was made to collect and mix light minerals with concentrations of heavy minerals. Many samples were collected at or adjacent to natural riffles or where good sediment traps existed.

Altered rocks sampled were either from bedrock in the summit areas of the four major cones or from random float material in landslide, colluvium, or reworked glacial deposits. Such float material is assumed to represent the higher altered-bedrock parts of the study area.

The main aspects of mineral-deposit trace-element distribution in the study area are summarized below, and details are shown on accompanying maps and tables. These analyses in general corroborate the field-geologic appraisal of an absence of significant mineral deposits.

Precious Metals (gold and silver).--No precious metals were detected in any samples at sensitivity levels of 0.7 ppm for silver and 0.05 ppm for gold.

Base Metals (lead, zinc, and copper).--The highest lead and zinc contents obtained are barely above background. In most samples, lead and zinc were not detected in the initial spectrographic scans. Samples with lead contents as great as 20-30 ppm are rare (fig. 17). The highest highest lead content (225 ppm) was found in a sample (LDA-103) with secondary copper-bearing minerals on a fracture coating in an andesite flow. Another similar sample (LDA-104) contained 70 ppm lead. A "soil" sample (LDA-048) contained 150 ppm.

Fig. 17.--near here

Zinc was detected during routine emission spectrographic analysis in only one sample (LDA-103), which contained visible copper minerals. Subsequent atomic-absorption analyses of selected samples (table 8) showed zinc contents ranging from 8 to 283 ppm in unaltered volcanic rocks or fracture coatings, stream sediments, and soils. There is little difference in the average zinc content of the different types of samples. Background values for Mt. Shasta are considered to be less than 70 ppm, lower than for mafic igneous rocks in general, given as 130 ppm by Hawkes and Webb (1962, p. 376).

Table 8--near here

Four of 26 samples of altered rocks or fracture coatings contain zinc contents above local background (table 8). The data indicate that zinc is low everywhere; even the highest of the four anomalous values is only 283 ppm, and it was obtained from a sample carrying secondary copper minerals in veinlets. Seven of 15 stream-sediment samples contain zinc above background. Five of the seven lie in the southeastern quadrant of the study area (fig. 17), in the Mud Creek drainage, which is the most deeply eroded part of Mt. Shasta and has the highest proportion of altered and mineralized rocks. Only one soil sample (LDA-049) of a total of 6 contains zinc above the 70 ppm background; the sample locality lies just south of the Wilderness Study Area and, like the stream-sediment samples with relatively high zinc, is the Mud Creek drainage.

Copper was detected in a number of samples during the routine spectrographic scan, and in others during subsequent atomic-absorption analyses (table 9). Background copper values lie below about 32 ppm. One-half of 26 samples of altered volcanic rocks or fracture coatings contain no more than background copper, and most of the rest contain no more than 62 ppm. Samples with the highest values come from the north end of Sargents Ridge and upper Mud Creek; the two highest are from samples with fracture coatings of secondary copper minerals. Most of the relatively high values are from the southeastern quadrant of the study area (fig. 18) in a belt trending north from near Red Butte to the summit of Mount Shasta. In the Sargents Ridge-upper Mud Creek area sparse bedrock and float samples are found containing secondary copper minerals such as malachite, azurite, and chrysocolla(?). Two samples (LDA-103 and -104) were collected from coatings along minor fractures and as disseminated minerals within a few centimeters of the fractures.

Table 9.-- near here

Fig. 18.-- near here

Stream-sediment samples generally contain only background copper values; one sample (LDA-014) having 34 ppm copper, is slightly above the somewhat arbitrarily defined background threshold and also came from near Sargents Ridge. The copper content of sampled soils is not especially great; the highest value is 48 ppm, and the 3 of 5 samples with above-background copper are from widely scattered localities.

Arsenic and antimony.--Arsenic and antimony can be useful geochemical indicators of precious metals, and arsenic commonly is associated with copper and cobalt in sulfide deposits (Hawkes and Webb, 1962). In the Mount Shasta Wilderness Study Area, arsenic and antimony in all analyzed samples are below the limit of detectibility by the emission spectrographic method. More sensitive analytical methods were used on 51 samples, atomic-absorption for arsenic and rhodamine B for antimony (fig. 19).

Fig. 19--near here

Only 6 of the 51 samples contain more than 2.4 ppm arsenic, which is considered to be background threshold. All the arsenic values are low. By far the highest, 24 ppm in sample no. LDA-048 is from a very small area of friable altered regolith material in the Misery Hill summit dome. This sample also contains the highest antimony (0.9 ppm) of any sample. Antimony in the 51 samples ranges from <0.1 to 0.9 ppm; 7 samples contain values slightly above the background of 0.4 ppm. Four altered volcanic rocks have slightly anomalous quantities of both arsenic and antimony. Most samples with arsenic or antimony above background lie near the central vents of the four main cones of Mt. Shasta, particularly on the Sargents Ridge cone.

Other metals (Mo, Bi, Sn, Be, Hg, Ni, Cr and V).--Slightly high amounts of molybdenum were found in several samples collected in the summit areas and in the Mud Creek drainage. Five of the determined values of molybdenum are considered to be barely above background for the area, ranging from 3 to 10 ppm (fig. 18). Repeat analyses on four other samples with 3-5 ppm molybdenum did not detect any of the metal. The sample with the highest content (10 ppm, LDA-096) came from a mildly altered dacite in the Brewer Creek drainage. Nearby samples of similar rocks contained only background amounts of molybdenum. A "soil" sample (LDA-048) with relatively high molybdenum was collected in the summit area of Shastina. This sample also contains the only detectable bismuth (10 ppm), as well as one of the highest lead, arsenic, and antimony values of all the samples. The "soil" is actually intensely decomposed and argillized rock from an inactive fumarolic area. Tin was detected at 20 ppm in a single sample bearing visible disseminated specularite, an amount well above the average of 6 ppm in mafic igneous rocks (Hawkes and Webb, 1962, p. 373). About a dozen samples carried detectable beryllium, which generally did not exceed 2 ppm (table 10, fig. 21). The background value is considered to extend up to about 3 ppm, because Be in several unaltered rock samples approaches this limit. Lanthanum was detected in four float rock samples from the Sargents Ridge area at 20 to 30 ppm; three unaltered rock samples also contained about 22-25 ppm La. The amounts are slightly high for the study area, but are within background values for volcanic rocks (Hawkes and Webb, 1962, p. 367). Ten samples of rock carry relatively high amounts of mercury, ranging from about 0.10 to 0.40 ppm (fig. 20). Nearly all the samples

Table 10-- near here

Fig. 20.-- near here

with relatively high mercury are associated with the central-vent areas near the summits of Shasta and Shastina, where anomalously high contents of other metallic elements are noted and where boron was also detected. The mercury as well as boron probably relate to fumarolic or thermal-spring activity. Numerous samples contain slightly high quantities of nickel and chromium (table 6, fig. 21); vanadium (table 6, fig. 21) is present in quantities as large as 700 ppm. All these values for chromium, nickel, and vanadium are background amounts, but some are slightly high backgrounds.

Fig. 21--near here

Nonmetallic deposits.--Of the nonmetallic elements, boron proved the most interesting. Twelve samples yielded 30 or more ppm, and five of these samples contained 100-250 ppm (fig. 22, table 11). These are all associated with vent areas near the summits of the four cones of Mt. Shasta and probably relate directly to thermal-spring or fumarolic activity. However boron does not occur on the mountain in large volumes or high concentrations. Sulfur is present in megascopic quantities around a few of the known thermal springs, where it has precipitated in a crystalline form admixed with siliceous sinter.

Fig. 22--near here

Table 11--near here

Conclusions.--The results of geochemical-exploration sampling in the Mt. Shasta Wilderness Study Area reflect alteration patterns related mainly to the central-vent areas of the four major volcanic cones. Samples with relatively high amounts of trace metals are mostly clustered in (or derived from) these altered areas. None of the trace metals analyzed are exceptionally high in concentration, but they do suggest a spotty low-grade mineralization of the volcanic centers. No orebodies of metallic minerals are likely to be present.

Rocks beneath the study area, even at considerable depth, are almost entirely parts of the volcanic complex of Mount Shasta. Metallic mineral deposits are no more likely to be concealed at depth than to occur at the surface. It is not possible to discount the presence of buried nonmetallic deposits, but the low value per production unit of the kinds of industrial minerals likely to occur makes economic recovery of buried nonmetallic deposits infeasible.

Economic Mineral Appraisal

The Mount Shasta Wilderness Study Area has been prospected for mineral deposits by prospectors, but no commercial-grade material has been found. Volcanic-cinder deposits just outside the area have been mined for many years, but almost none occur within it. Sulfur occurs around fumaroles on the summit dome of Mount Shasta but is not in sufficient amounts to be a resource.

Three unpatented placer claims, located primarily for platinum, are in, or partially within, the study area. The claims have been ~~are~~ inactive since 1956. Samples from them contained no platinum. None of the world's commercial platinum deposits is known to occur in a similar geologic environment.

Sampling and Analytical Techniques.--Twenty four grab or random chip samples were taken from the claimed areas. No mineralized structures were observed on any of the claims. All samples were analyzed for gold, silver, platinum, and checked for radioactivity and fluorescence. Seven were analyzed by semiquantitative spectrographic methods for 43 elements.

Mining Claims.--Courthouse records at Yreka, California, show that three placer claims were located at least partly within the study area (fig. 23). The three claims, located in 1924, 1925, and 1956, cover 480 acres (194 h) or 160 acres (65 h) each. No prospect pits or mine workings were observed on any of the claims. No lode claims were found in the area.

Fig. 23--near here

Name: Glacier No. 1 placer

Index Map No.: 1-A and 1-B

Location: This claim consists of two parcels, 6 miles (9.7 km) apart. One parcel, 1-A, is in the study area on the west boundary. The second parcel, 1-B, is about 1 mile (1.6 km) east of the boundary.

Elevation: Parcel 1-A at 9,000 to 10,000 feet (2,743 to 3,048 m), 1-B at 6,000 feet (1,829 m).

Access: Logging roads within 1.25 miles (2 km) of parcel 1-A, and cross parcel 1-B.

History: Claim located by G. H. Thompson, Nov. 3, 1924, for platinum.

Previous production: None

Geology of deposit: Parcel 1-A - rhyolite, dacite, andesite, and tuffs ranging in color from dark gray to light reddish brown. Parcel 1-B - light-gray to dark-gray andesite and light-gray pumice. No mineralized rock observed.

Development: None

Sampling: Eight samples were taken from outcrops and float on parcel 1-A and two samples were taken from outcrops at parcel 1-B. The samples contained no platinum or other metallic values.

Conclusions: The property has no economic mineral potential.

Name: Glacier No. 2 placer

Index Map No.: 2

Location: The claim is near the east boundary, within the study area.

Elevation: 7,000 to 7,600 feet (2,134 to 2,316 m).

Access: Logging roads within one-fourth mile (0.4 km) of claim.

History: Claim located by G. H. Thompson, Jan. 12, 1925, for platinum.

Previous production: None

Geology of deposit: Light-gray to dark-gray andesite. No mineralized rock observed.

Development: None.

Sampling: Three samples taken from rock exposed contained no platinum or other metallic values.

Conclusions: The property has no economic mineral potential.

Name: Lotus placer

Index Map No.: 3

Location: The claim is mostly outside the southern boundary of the study area.

Elevation: 7,700 to 9,800 feet (2,347 to 2,987 m).

Access: Paved road to ski lodge located on claim.

History: Claim located by Thomas D. Chace, September 23, 1956, for platinum.

Previous production: None

Geology of deposit: Glacial outwash and moraines consisting of rhyolite, dacite, and andesite. No mineralized rock observed.

Development: Ski area

Sampling: Twelve samples taken of float contained no platinum or other metallic values.

Conclusions: The property has no economic mineral potential.

REFERENCES CITED

Albers, J. P., 1966, Economic deposits of the Klamath Mountains, in Bailey, E. H., ed., Geology of northern California: Calif. Div. Mines and Geology Bull. 190, p. 51-62.

Anderson, A. T., Jr., 1974, Evidence for a picritic volatile-rich magma beneath Mt. Shasta, California: Jour. Petrol., v. 15, p. 243-267.

Blakely, R. J., and Christiansen, R. L., 1976, The magnetization of Mt. Shasta [abs]: Am. Geophys. Union Trans. (EOS), v. 57, p. 903.

Chapman, R. H., and Bishop, C. C., 1967, Bouguer gravity map of California, Alturas sheet: Sacramento, Calif. Div. Mines and Geol.

Chesterman, C. W., 1956, Pumice, pumicite, and volcanic cinders in California: Calif. Div. Mines Bull. 174, 119 p.

Christiansen, R. L., and Miller, C. D., 1976, Volcanic evolution of Mt. Shasta, California: Geol. Soc. America, Abstracts with Programs, v. 8, no. 3, p. 360-361.

Clark, W. B., 1966, Gold in Mineral and water resources of California: Pt. 1: Committee Print. 89th Congress, 2d session, 450 p.

Condie, K. C., and Swenson, D. H., 1973, Compositional variation in three Cascade stratovolcanoes: Jefferson, Rainier, and Shasta: Bull. Volc., v. 37-2, p. 205-230.

Crandell, D. R., 1971, Postglacial lahars from Mount Rainier Volcano, Washington: U.S. Geol. Survey Prof. Paper 677, 75 p.

Crandell, D. R., 1973, Hot pyroclastic-flow deposits of probably Holocene age west of Mount Shasta volcano, California: Geol. Soc. America, Abstracts with Programs, v. 5, no. 1, p. 28.

Crandell, D. R., and Mullineaux, D. R., 1975, Technique and rationale of volcanic-hazards appraisals in the Cascade Range, Northwestern United States, in Environmental Geology: New York, Springer-Verlag, p. 23-32.

Eichelberger, J. C. 1975, Banded andesitic bombs of Mt. Shasta, California: Geol. Soc. America, Abs. with Programs, v. 7, no. 7, p. 1065-1066.

Finch, R. H., 1930, Activity of a California volcano in 1786: Volcano letter, no. 308, p. 3.

Gay, T. E., Jr., 1966, Economic mineral deposits of the Cascade Range, Modoc Plateau, and Great Basin region of northeastern California, in Bailey, E. H., ed., Geology of northern California: Calif. Div. Mines and Geol. Bull. 190, p. 97-104.

Harrison, C. G. A., Jarrard, R. D., Vacquier, V., and Larson, R. L., 1975, Paleomagnetism of Cretaceous Pacific seamounts: Geophys. J., v. 42, p. 859-882.

Hawkes, H. E., and Webb, J. S., 1962, Geochemistry in mineral exploration: Harper & Row, N. Y., 415 p.

Heiken, G., 1976, Depressions surround volcanic fields: A reflection of underlying batholiths?: Geology, v. 4, p. 568-572.

Irwin, W. P., and Bath, G. D., 1962, Magnetic anomalies and ultramafic rock in northern California, in Short Papers in the Geologic and Hydrologic Sciences: U.S. Geol. Survey Prof. Paper 450-B, p. B65-B67.

Kim, C. K., and Blank, H. R., Jr., 1972, Bouguer gravity map of California, Weed Sheet: Sacramento, Calif. Div. Mines and Geol.

LaFehr, T. R., 1965, Gravity, isostasy, and crustal structure in the southern Cascade Range: Jour. Geophys. Res., v. 70, p. 5581-5597.

Miller, C. D., and Crandell, D. R., 1975, Postglacial pyroclastic-flow deposits and lahars from Black Butte and Shastina, west of Mt. Shasta, California: Geol. Soc. America, Abstracts with Programs, v. 7, no. 3, p. 347-348.

Parker, R. L., 1967, Chapt. D. Composition of the earth's crust, in Data of Geochemistry, Sixth Ed.: U. S. Geol. Survey Prof. Paper 440-T, 19 p.

Peterman, Z. E., Carmichael, I. S. E., and Smith, A. L., 1970, Sr^{87}/Sr^{86} ratios of Quaternary lavas of the Cascade Range, northern California: Geol. Soc. America Bull., v. 81, p. 311-317.

Peters, L. J., 1949, The direct approach to magnetic interpretation and its practical application: Geophysics, v. 14, p. 290-320.

Plouff, D., 1975, Derivation of formulas and Fortran programs to compute magnetic anomalies of prisms: U.S. Dept. Commerce N.T.I.S. Rep. PB-243, 525 p.

Plouff, D., 1976, Gravity and magnetic fields of polygonal prisms and application to magnetic terrain corrections: Geophys., v. 41, p. 727-741.

Rankama, Kalervo and Sakama, Th. G., 1950, Geochemistry: Univ. Chicago Press, Chicago, 912 p.

Shapiro, L., 1975, Rapid analysis of silicate, carbonate, and phosphate rocks--revised edition: U.S. Geol. Survey Bull. 1401, 76 p.

Smith, A. L., and Carmichael, I. S. E., 1968, Quaternary lavas from the southern Cascades, Western U.S.A.: Contr. Mineral. and Petrol., v. 19, p. 212-238.

Smith, R. L., and Shaw, H. R., 1975, Igneous-related geothermal systems in White, D. E., and Williams, D. L., eds., Assessment of geothermal resources of the United States--1975: U.S. Geol. Survey Circ. 726, p. 58-83.

Steinborn, T. L., 1972, Trace element geochemistry of several volcanic centers in the High Cascades: Univ. Oregon, unpub. M. S. thesis.

Strand, R. G., compiler, 1963, Geologic map of California, Weed Sheet: Sacramento, Calif. Div. Mines and Geology.

Talwani, M., 1965, Computation with the help of a digital computer of magnetic anomalies caused by bodies of arbitrary shape: Geophysics, v. 30, no. 5, p. 797-817.

Vacquier, V., and Uyeda, S., 1967, Paleomagnetism of nine seamounts in the western Pacific and of three volcanoes in Japan: Bull. Earthquake Res. Inst., v. 45, p. 815-848.

Williams, H., 1932, Mount Shasta, a Cascade volcano: Jour. Geol., v. 45, p. 417-429.

Williams, H., 1934, Mount Shasta, California: Zeitschr. Vulkan., v. 15, p. 225-253.

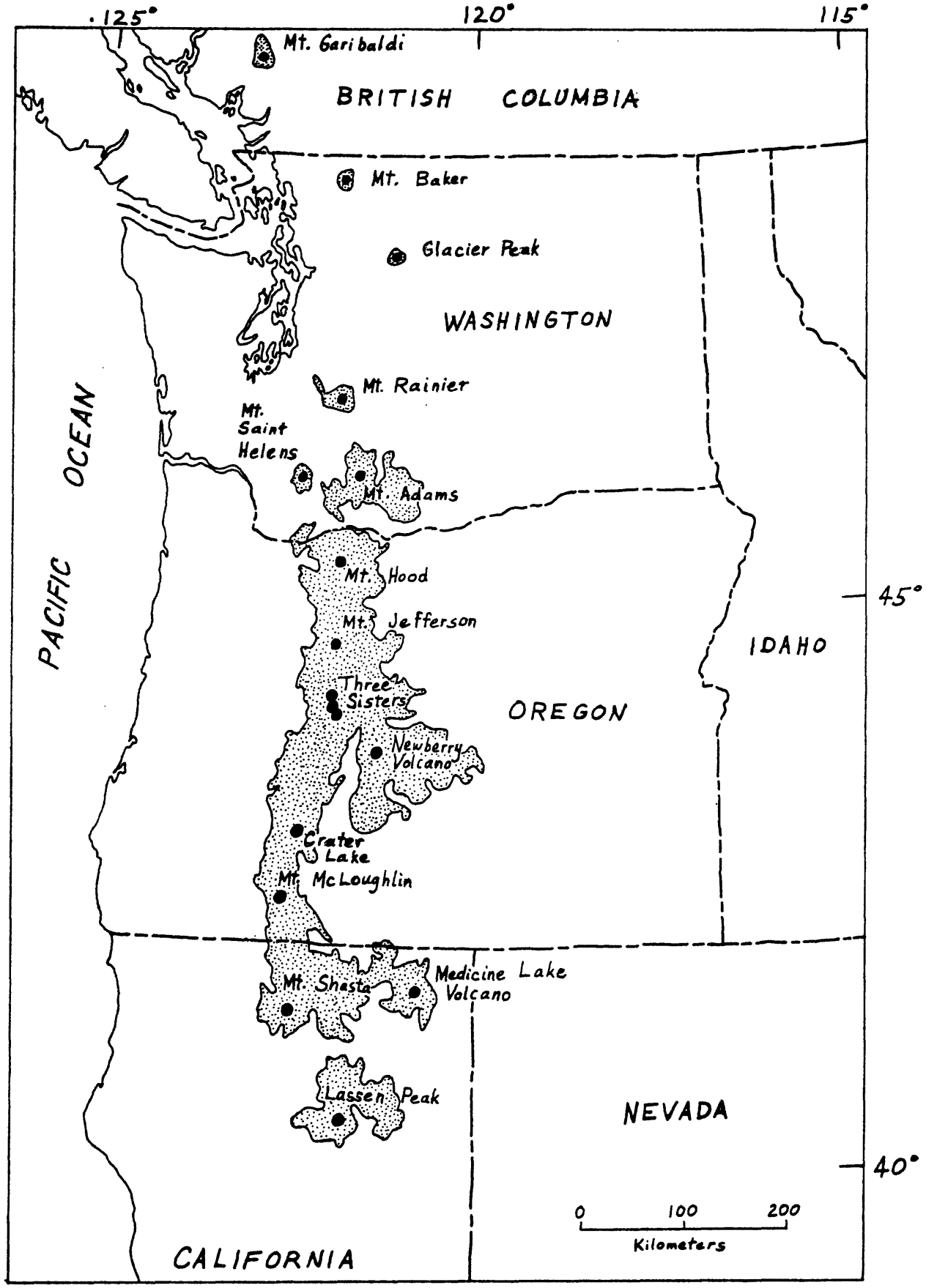
125°
120°
115°
Mt. Garibaldi
BRITISH COLUMBIA
Mt. Baker
Glacier Peak
WASHINGTON
Mt. Rainier
Mt. Saint Helens
Mt. Adams
PACIFIC OCEAN
Mt. Hood
Mt. Jefferson
Three Sisters
OREGON
Newberry Volcano
Crater Lake
Mt. McLoughlin
IDAHO
45°
Medicine Lake Volcano
Mt. Shasta
Lassen Peak
NEVADA
40°
0
100
200
Kilometers
CALIFORNIA

FIGURE 1

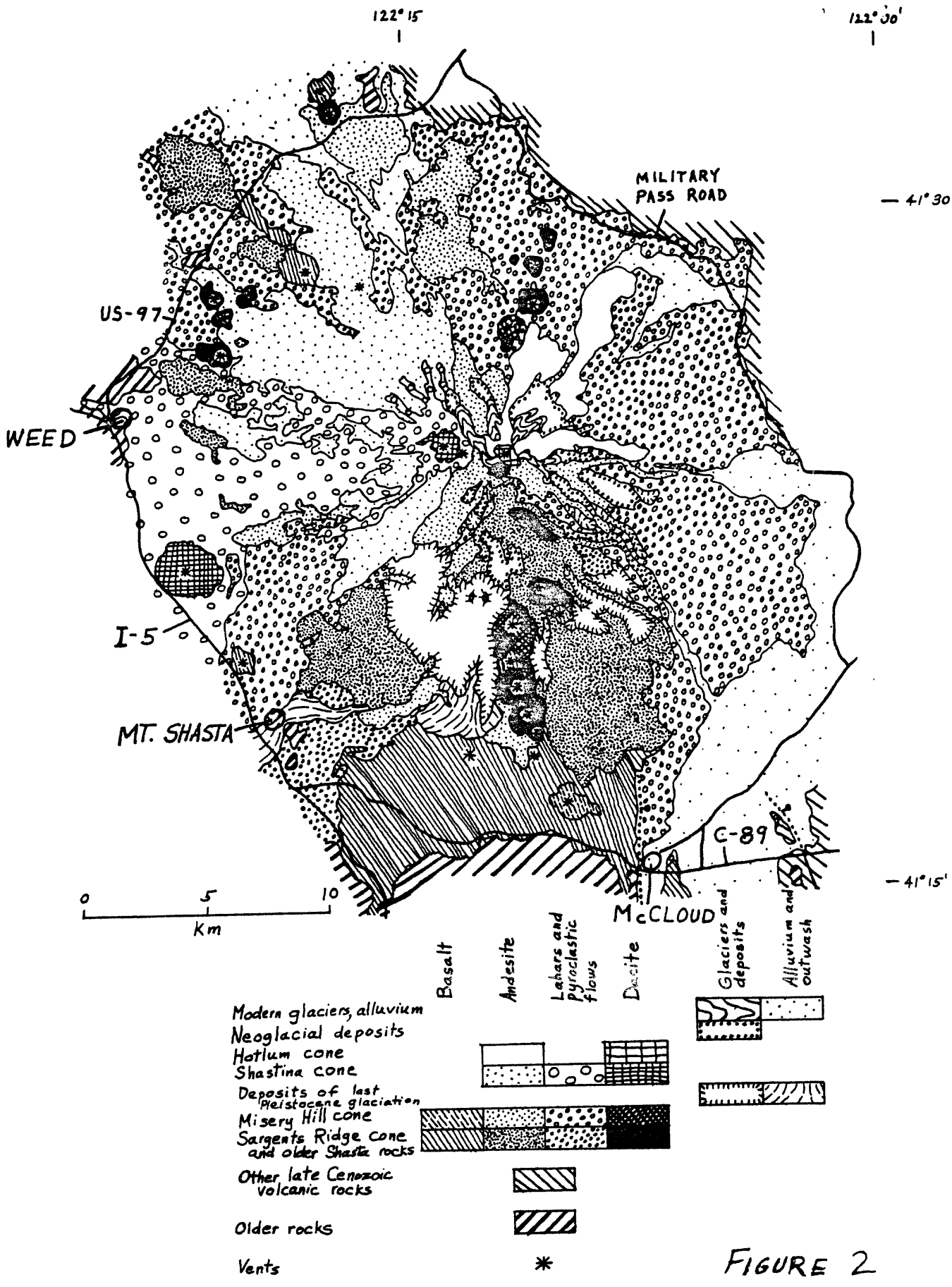
122° 15'
122° 30'
41° 30'
41° 15'
MILITARY PASS ROAD
US-97
WEED
I-5
MT. SHASTA
C-89
McCLOUD
0 5 10
Km
Basalt
Andesite
Lahars and pyroclastic flows
Dacite
Glaciers and deposits
Alluvium and outwash
Modern glaciers, alluvium
Neoglacial deposits
Hotlum cone
Shastina cone
Deposits of last Pleistocene glaciation
Misery Hill cone
Sargents Ridge cone and older Shasta rocks
Other late Cenozoic volcanic rocks
Older rocks
Vents

FIGURE 2

Figure 8.--Photograph of the Hotlum cone. Aerial view from the north showing lava flow from central vent emerging from beneath Hotlum Glacier. Summit is dome that fills the central-vent crater.

Figure 9.--Aeromagnetic map of the area surrounding Mount Shasta. Contours represent total field anomaly calculated by subtracting the IGRF regional field updated to 1975. Contour interval is 20 gammas, and flight altitutde was 2,600 m above sea level.

Figure 10.--Aeromagnetic map of Mount Shasta. Contours represent total field anomaly calculated by subtracting the IGRF regional field updated to 1975. Contour interval is 5 gammas, and flight altitude was 4,400 m above sea level.

Figure 11.--Digitized approximation to the topography of Mount Shasta. Numbers identify layers. Elevations in feet of the tops of the layers, in order of increasing layer number, are 14,080, 13,920, 13,600, 13,200, 12,800, 12,400, 12,000, 12,240, 12,240, 12,000, 11,600, 11,200, 10,800, 10,000, and 9,200. The four X symbols locate the corners of the residual map of Figure 12.

Figure 12.--Residual field resulting from inverse model of Mt. Shasta aeromagnetic data using layers 1 through 15 of figure 11. Contour interval is 25 gammas. Plus symbols show the location of field points used in the inversion.

Figure 13.--Digitized approximation of the topography of Ash Creek Butte. Numbers identify layers. Elevations in feet of the tops of the layers, in order of increasing layer number are 8,240, 8,000, 7,600, 7,600, 7,200, 6,800, 6,400, and 6,000. The four X symbols locate the corners of the residual map of Figure 14.

FIGURE CAPTIONS

Figure 1.--Index map showing Mt. Shasta in relation to the Cascade chain. Stipple, Quaternary volcanic rocks of the Cascade Chain.

Figure 2.--Generalized geologic map of Mt. Shasta.

Figure 3.--Geologic map of the Mt. Shasta Wilderness Study Area.

Figure 4.--Bouguer gravity map of Mt. Shasta and the surrounding region. After LaFehr (1965), Chapman and Bishop (1967), and Kim and Blank (1972).

Figure 5.--Photograph of Sargents Ridge and upper Mud Creek. Aerial view northward across the eroded crater of the Sargents Ridge cone, overlapped at head of Mud Creek by flows of the Misery Hill cone. Ridge left of center is Sargents Ridge; point at upper end of Sargents Ridge, profiled against Konwakiton Glacier, is Thumb Rock. Lavas and breccias beneath Thumb Rock dip away from the camera toward the summit of Mt. Shasta.

Figure 6.--Photograph of Misery Hill, upper Avalanch Gulch, and the Mt. Shasta summit. Aerial view northeastward showing eroded crater rim of Misery Hill cone on the left. Misery Hill, below the summit snowfield and left of the large southeast-facing snowfield, is a dome within the Misery Hill crater, mantled by pumice flows of the Red Banks.

Figure 7.--Photograph of Shastina and the Mt. Shasta summit. Aerial view from the northwest showing cone of Shastina (foreground, just below horizon); the Whitney Glacier, just behind, lies between the Mt. Shasta summit and the erosionally breached crater rim of the Misery Hill cone. Prominent oblique line on the slope of Shastina just above timberline is margin of flow from the Shastina central vent deflected westward by high levees of older Shastina flow.

FIGURE 6

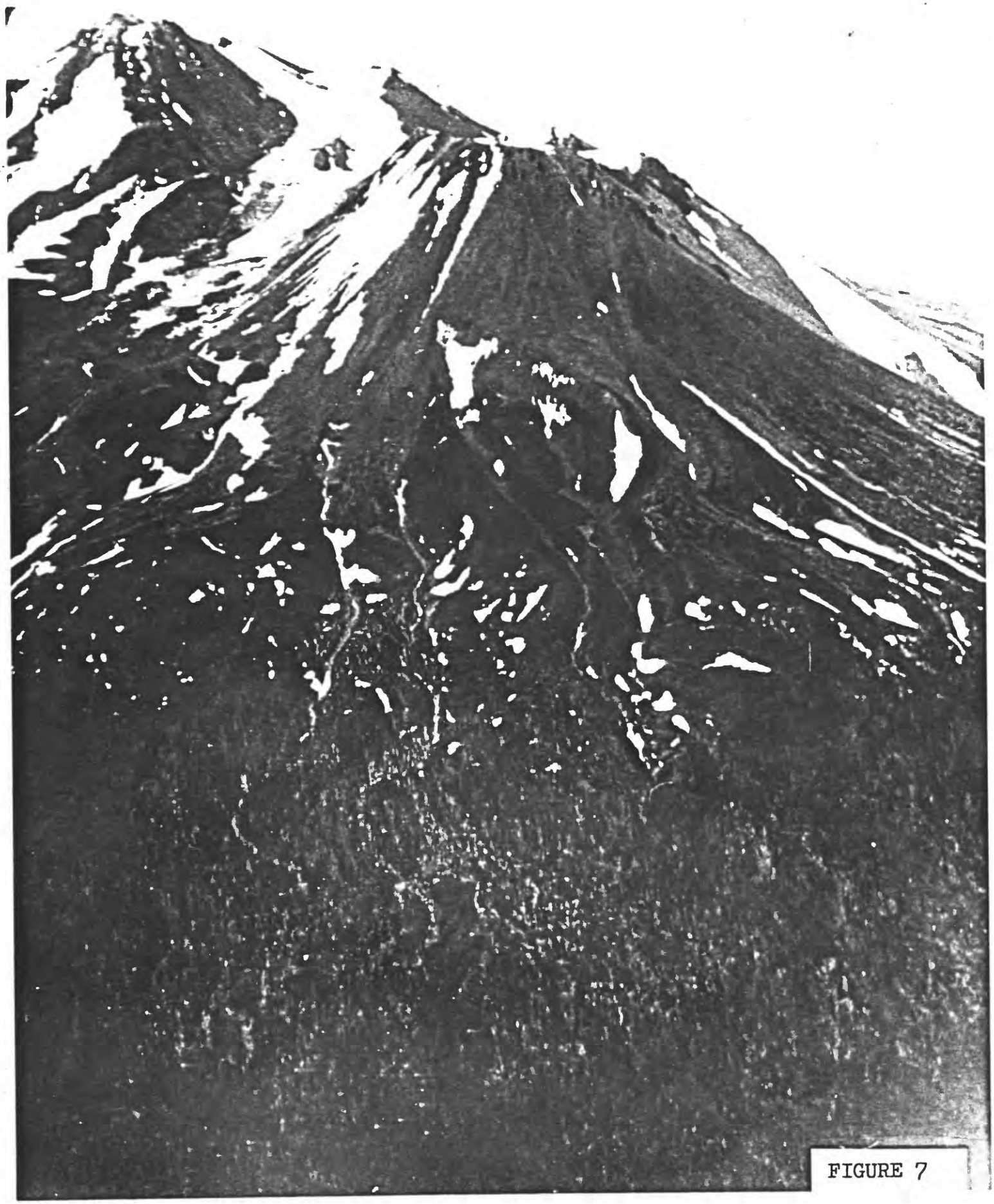

FIGURE 7

FIG. 9

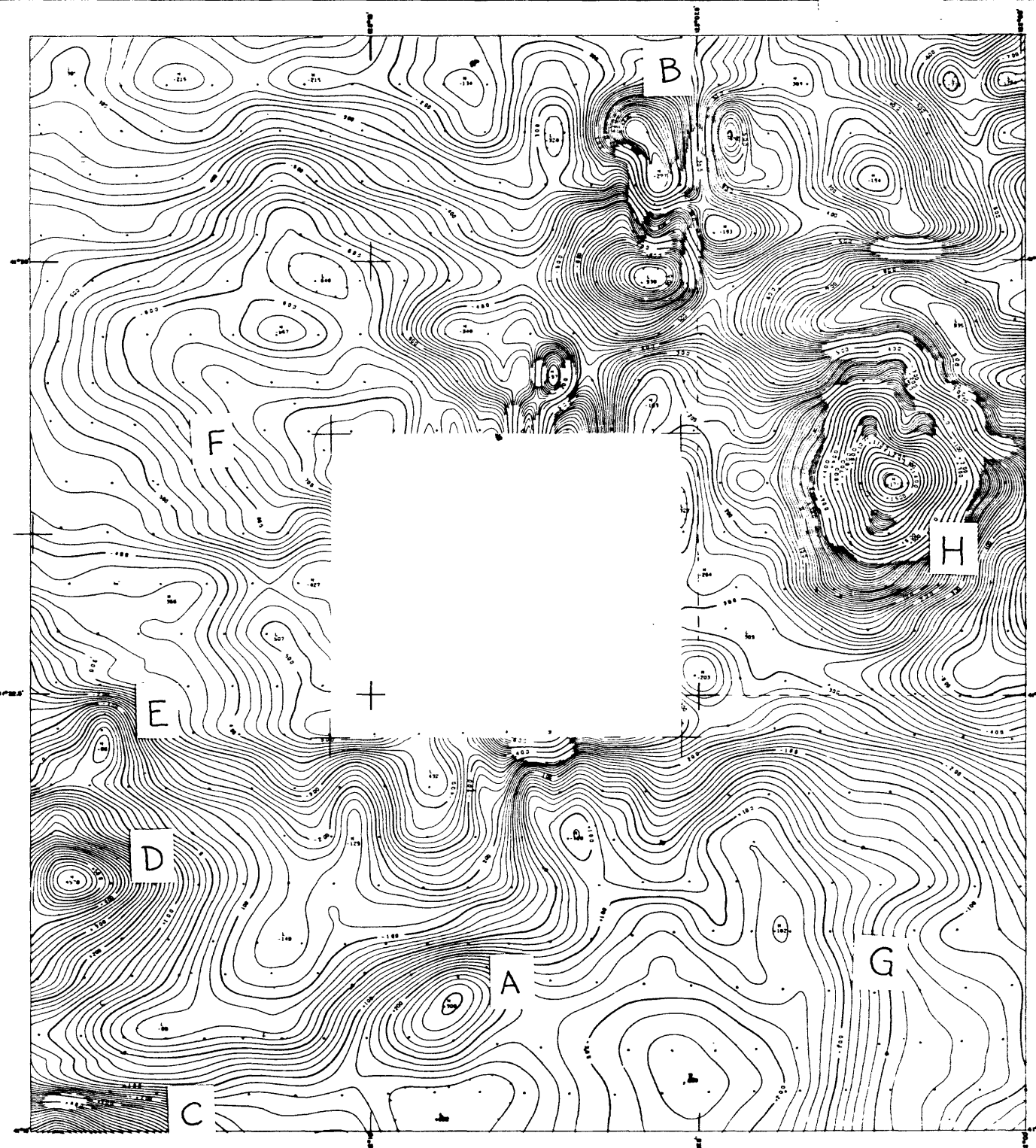

EXPLANATION

MAGNETIC CONTOURS SHOWING TOTAL INTENSITY MAGNETIC FIELD OF THE EARTH IN GAMMAS RELATIVE TO AN ARBITRARY DATUM. HACHURE TICKS INDICATE AREAS OF LOWER INTENSITY.

A REGIONAL TREND OF 775 GAMMAS/MILE NORTH AND 440 GAMMAS/MILE EAST WAS REMOVED USING 10,000 FT. UPDATED TO JULY 1975. MAP SHOWS ORIGINAL COMPUTER DRAWN CONTOURS

DATUM BASE OF 30,291.0 AT LOWER LEFT HAND CORNER

FLIGHT PATH SHOWING LOCATION AND SPACING OF DATA

AEROMAGNETIC MAP

0 1 2 3 4 5 MILES

CONTOUR INTERVAL	20 GAMMAS
FLIGHT LINE SPACING	ONE MILE
FLIGHT ALTITUDE	8,500'
FLOWN & COMPILED	JULY 1975

AERIAL SURVEYS, S.L.C., UTAH

APPROX. MAGNETIC DECLINATION

RESIDUAL MAGNETIC INTENSITY

MT. SHASTA, CALIFORNIA

U.S. GEOLOGICAL SURVEY

AREA "A"

0 2 4

km

FIG. 11

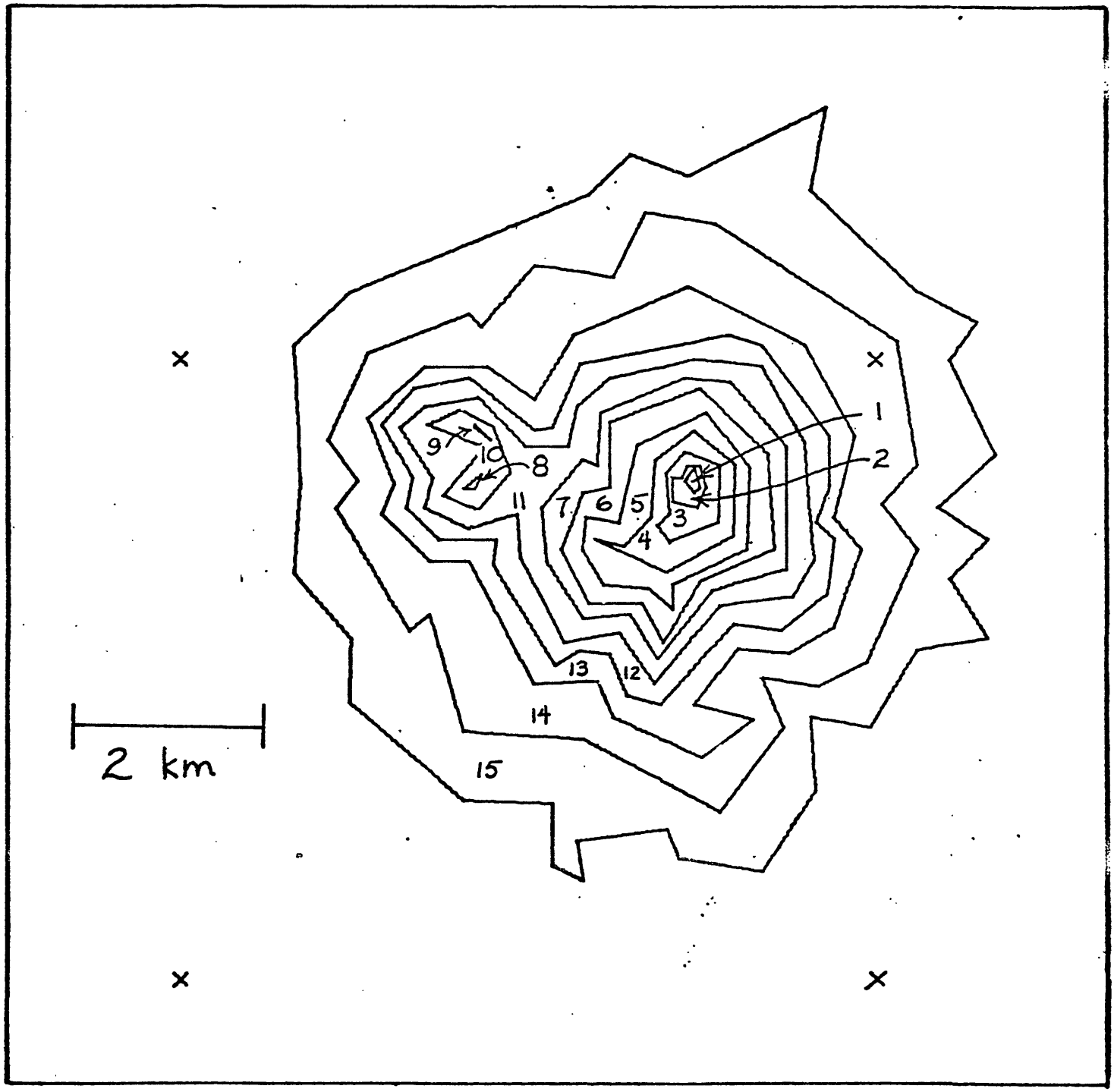

FIG. 10

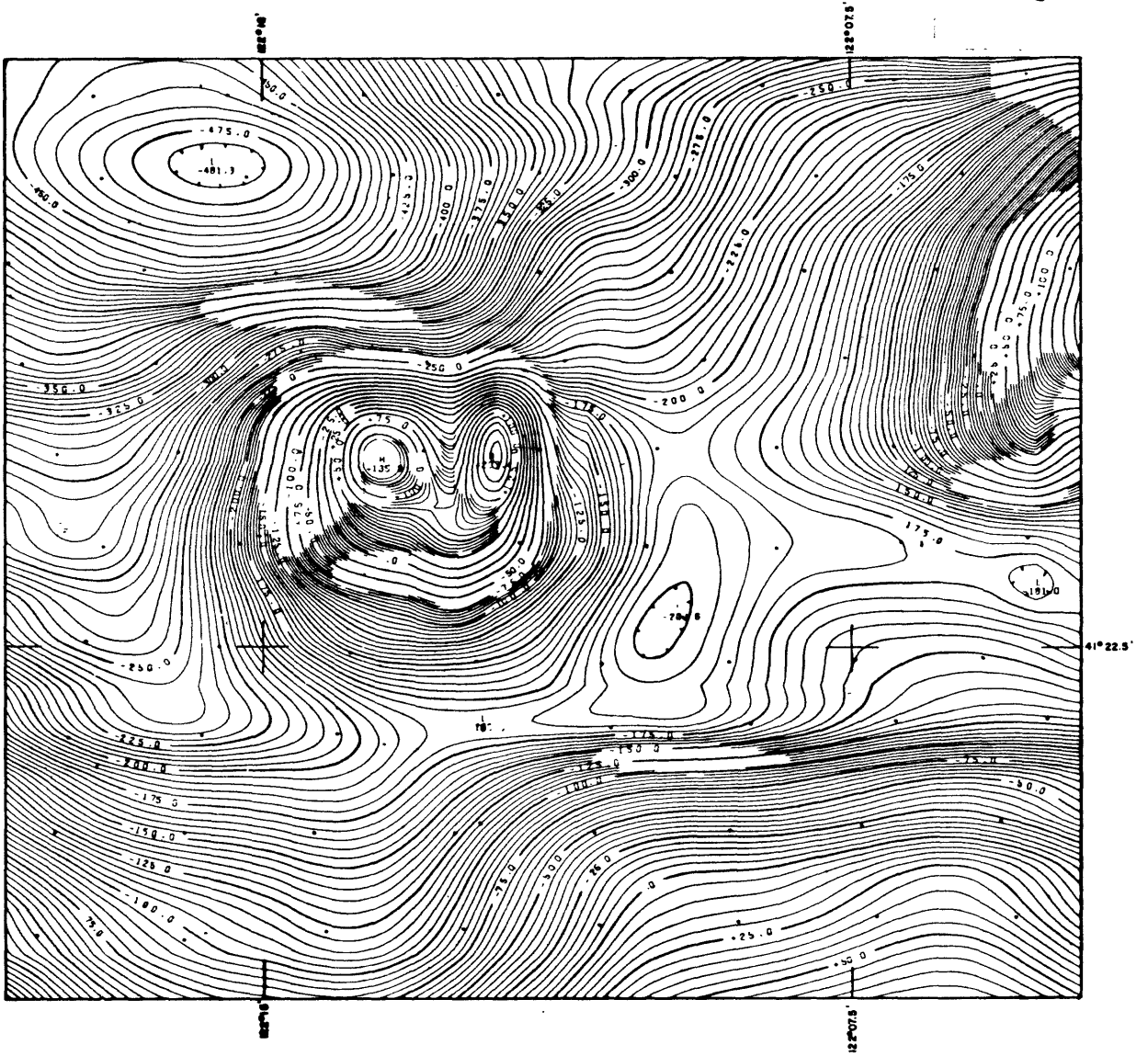

EXPLANATION

MAGNETIC CONTOURS SHOWING TOTAL INTENSITY MAGNETIC FIELD OF THE EARTH IN GAMMAS RELATIVE TO AN ARBITRARY DATUM. HACHURE TICKS INDICATE AREAS OF LOWER INTENSITY.

A REGIONAL TREND OF 7.72 GAMMAS/MILE NORTH AND 4.45 GAMMAS/MILE EAST WAS REMOVED USING I.G.R.F. UPDATED TO JULY 1975. MAP SHOWS ORIGINAL COMPUTER DRAWN CONTOURS.

DATUM BASE OF 53,389.4 AT LOWER LEFT HAND CORNER.

FLIGHT PATH SHOWING LOCATION AND SPACING OF DATA . . . .

AEROMAGNETIC MAP

1 0 1 2 3 MILES

CONTOUR INTERVAL	5 GAMMAS
FLIGHT LINE SPACING	ONE MILE
FLIGHT ALTITUDE	14,500'
FLOWN & COMPILED	JULY 1975

AERIAL SURVEYS, S.L.C., UTAH

TN MN 19°

APPROX. MAGNETIC DECLINATION

RESIDUAL MAGNETIC INTENSITY

SHASTA, CALIFORNIA

U.S. GEOLOGICAL SURVEY

AREA "A"

0 1 2 3

km

FIG. 12

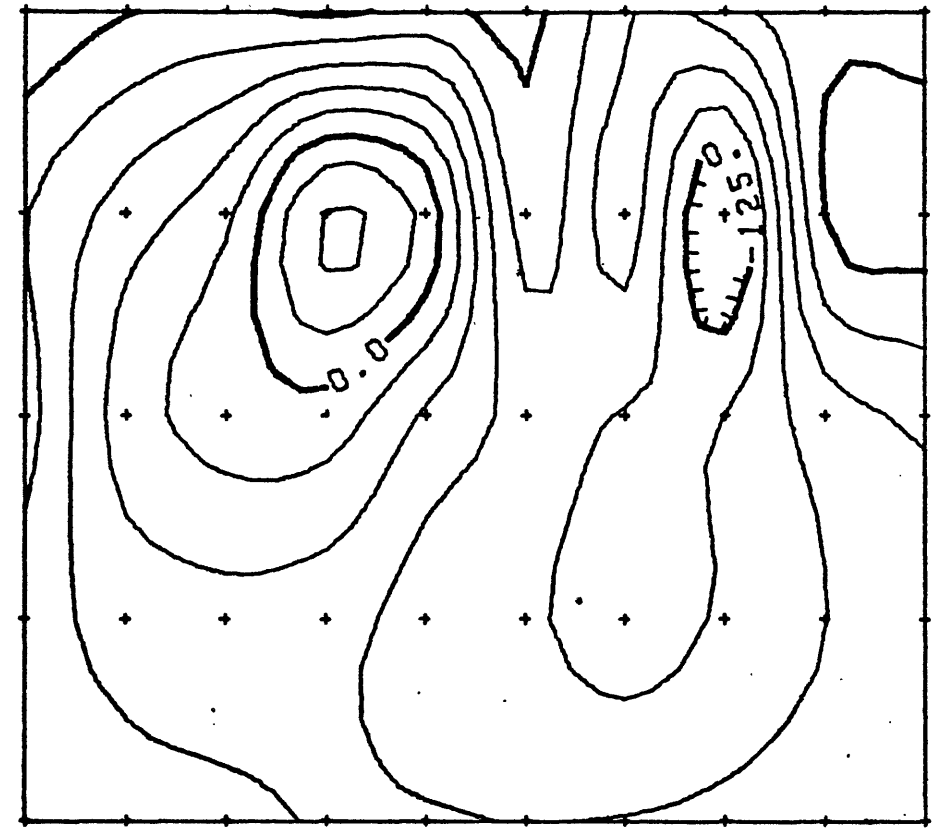

FIG. 13

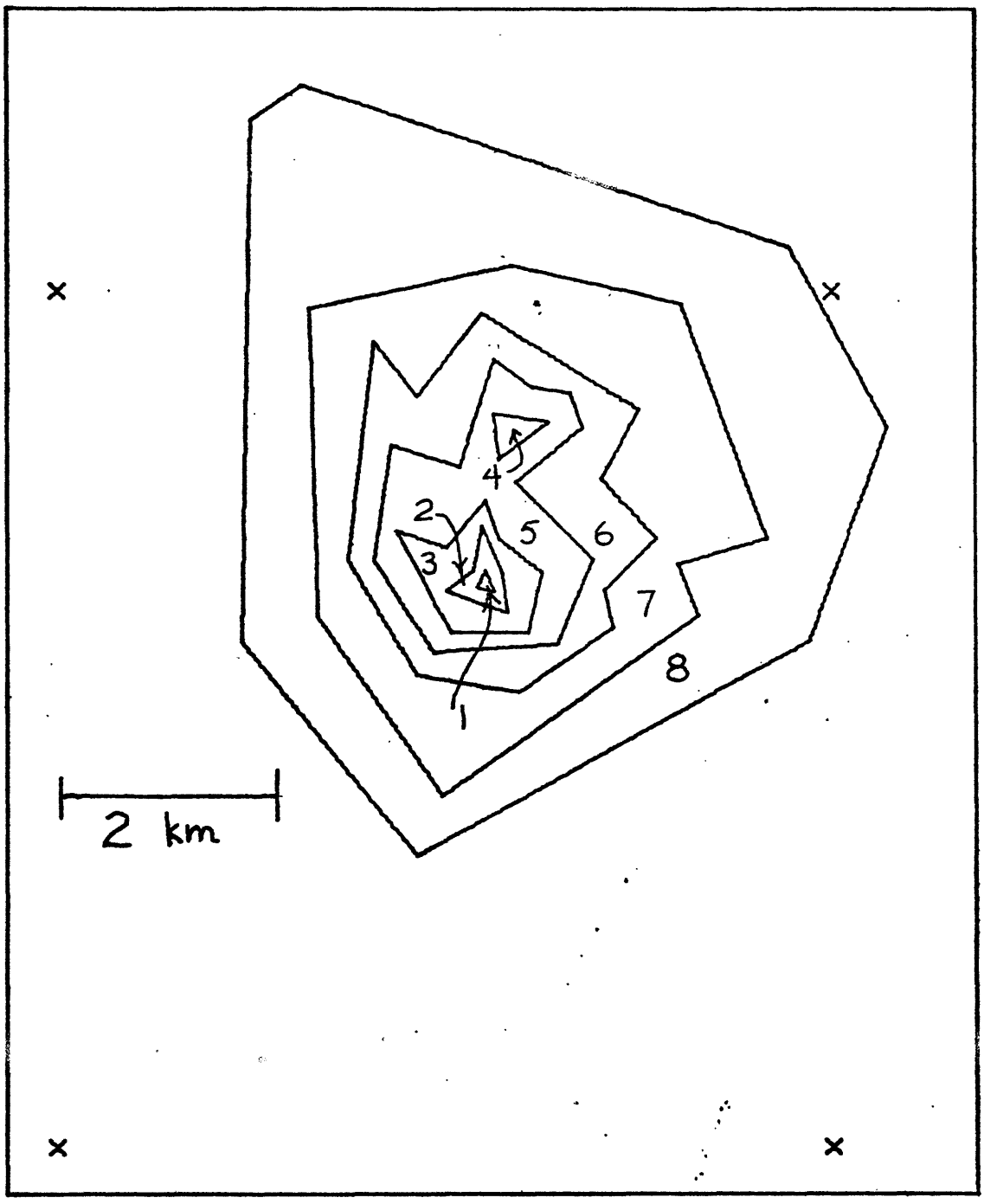

FIG. 14

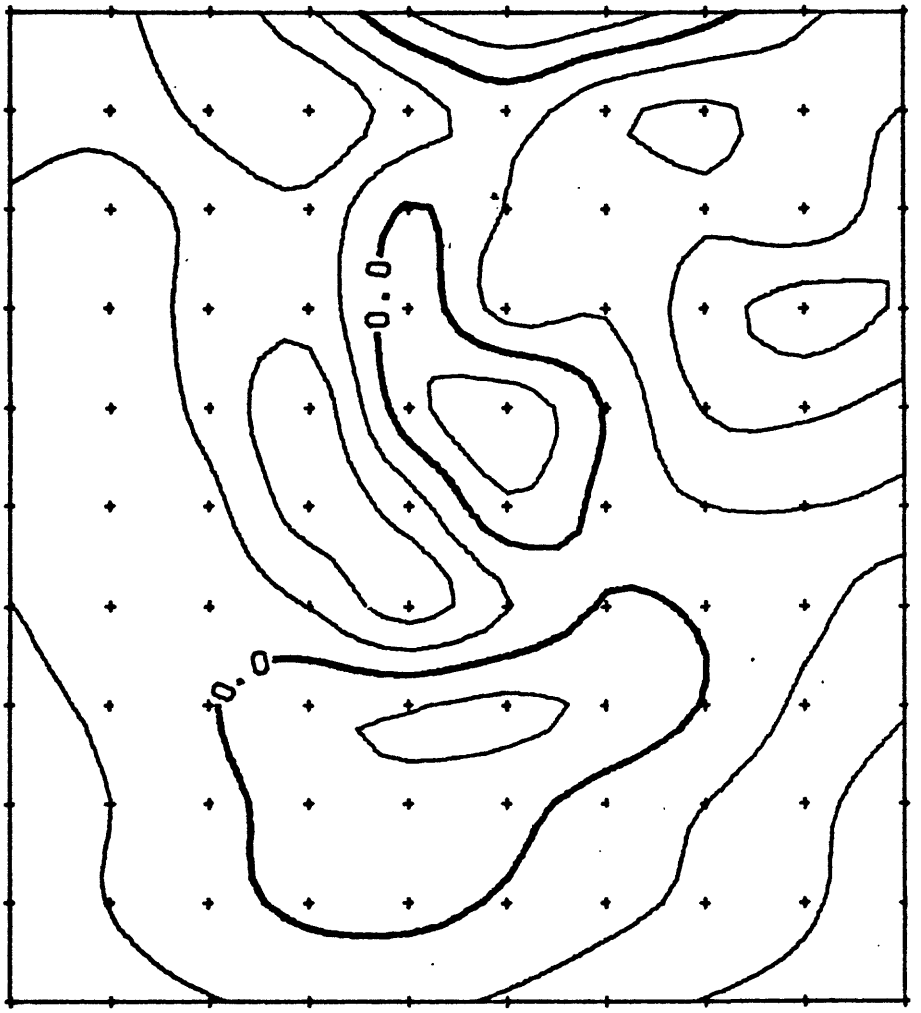

2 km

FIG. 15

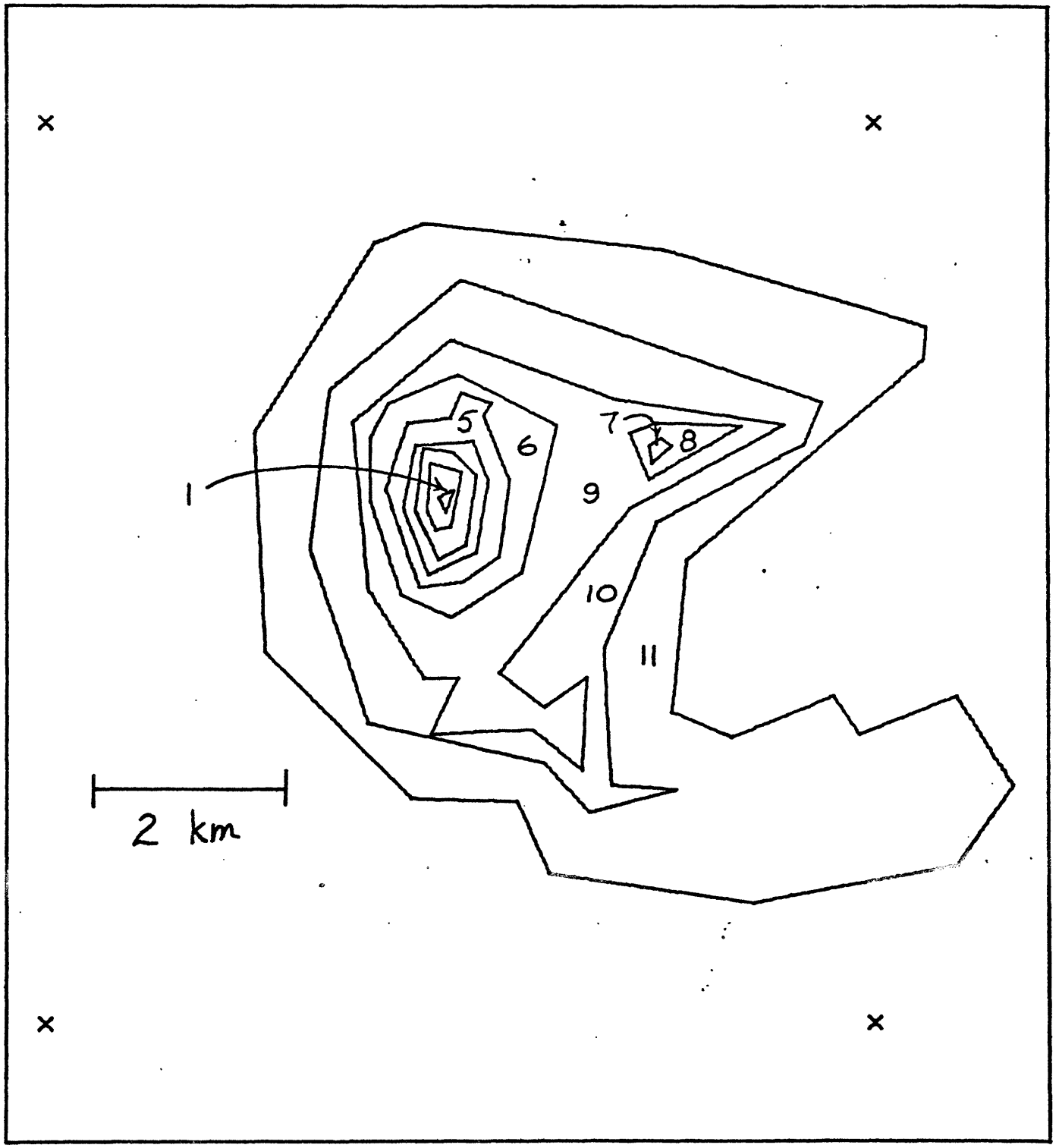

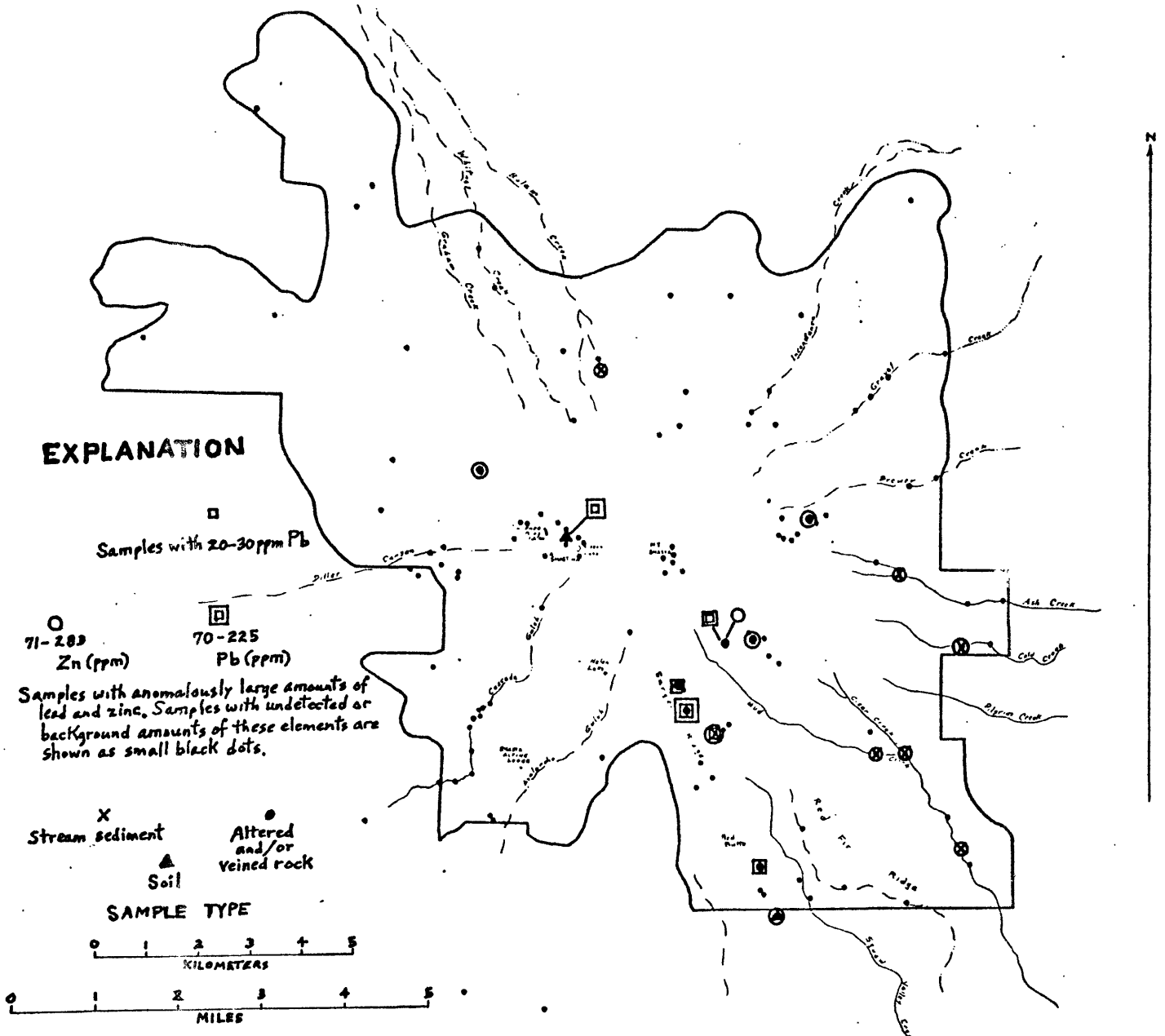
EXPLANATION
Samples with 20-30 ppm Pb
71-283
Zn (ppm)
70-225
Pb (ppm)
Samples with anomalously large amounts of lead and zinc. Samples with undetected or background amounts of these elements are shown as small black dots.
Stream sediment
Altered and/or veined rock
Soil
SAMPLE TYPE
0 1 2 3 4 5
KILOMETERS
0 1 2 3 4 5
MILES
N
Ash Creek
Pilgrim Creek
Red Fir Ridge

Fig. 17

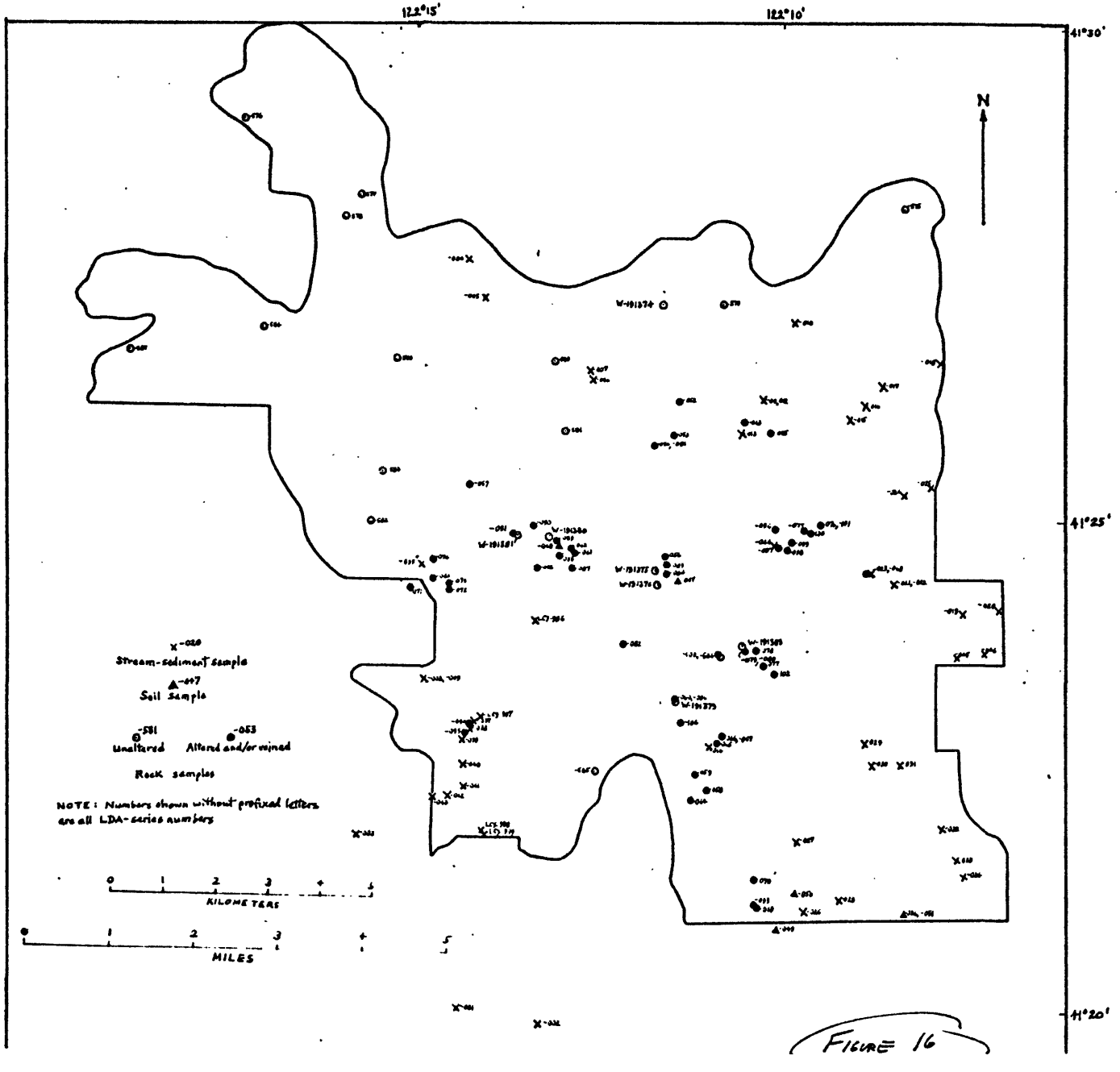
122°15'
122°10'
41°30'
41°25'
41°20'
N
Stream-sediment sample
Soil sample
Unaltered
Altered and/or mined
Rock samples
NOTE: Numbers shown without prefixal letters are all LDA-series numbers
0 1 2 3 4 5
KILOMETERS
0 1 2 3 4 5
MILES

FIGURE 16

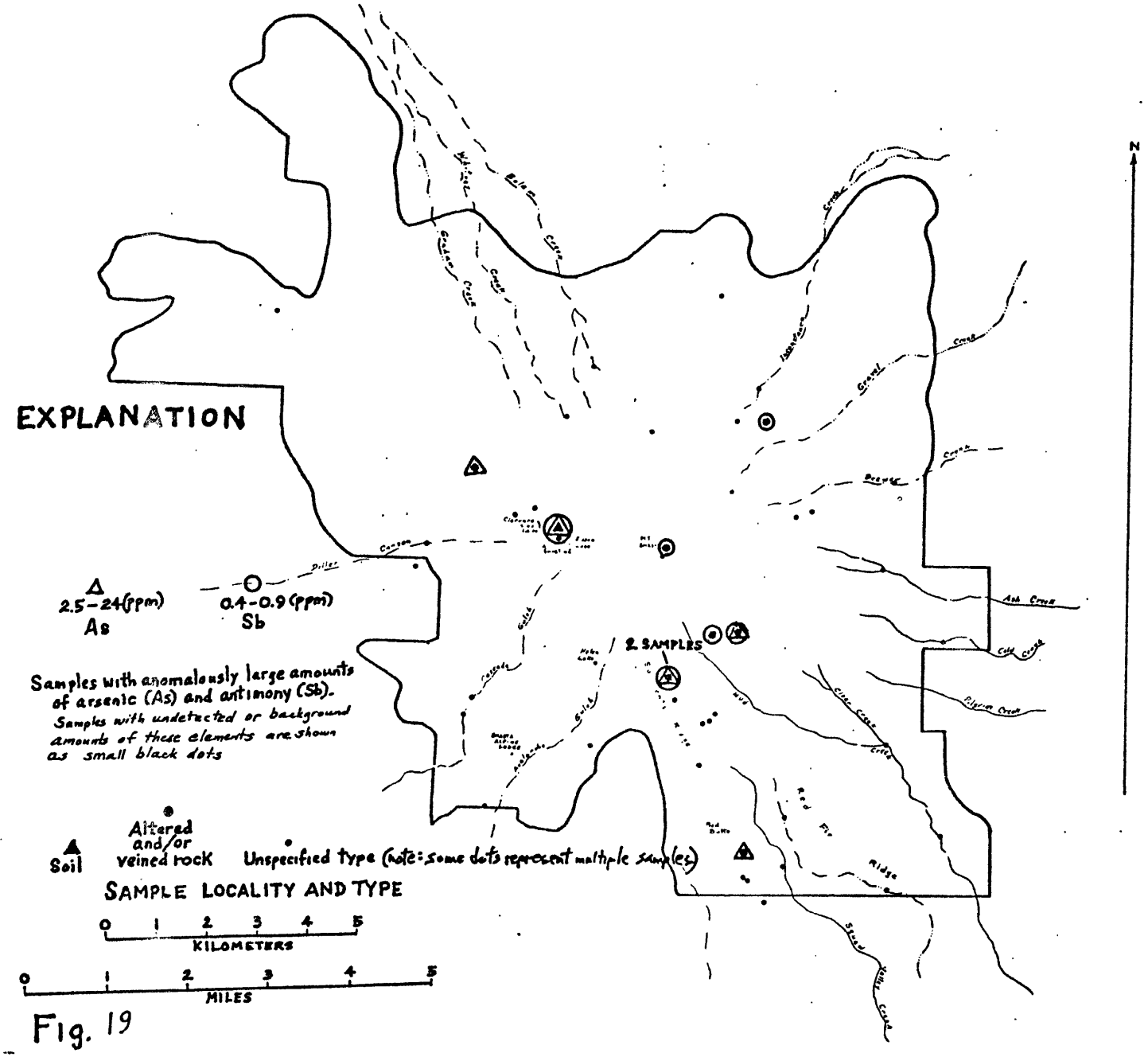
EXPLANATION
2.5–24 (ppm) As
0.4–0.9 (ppm) Sb
Samples with anomalously large amounts of arsenic (As) and antimony (Sb).
Samples with undetected or background amounts of these elements are shown as small black dots
2 SAMPLES
Soil
Altered and/or veined rock
Unspecified type (note: some dots represent multiple samples)
SAMPLE LOCALITY AND TYPE
0 1 2 3 4 5
KILOMETERS
0 1 2 3 4 5
MILES
N

Fig. 19

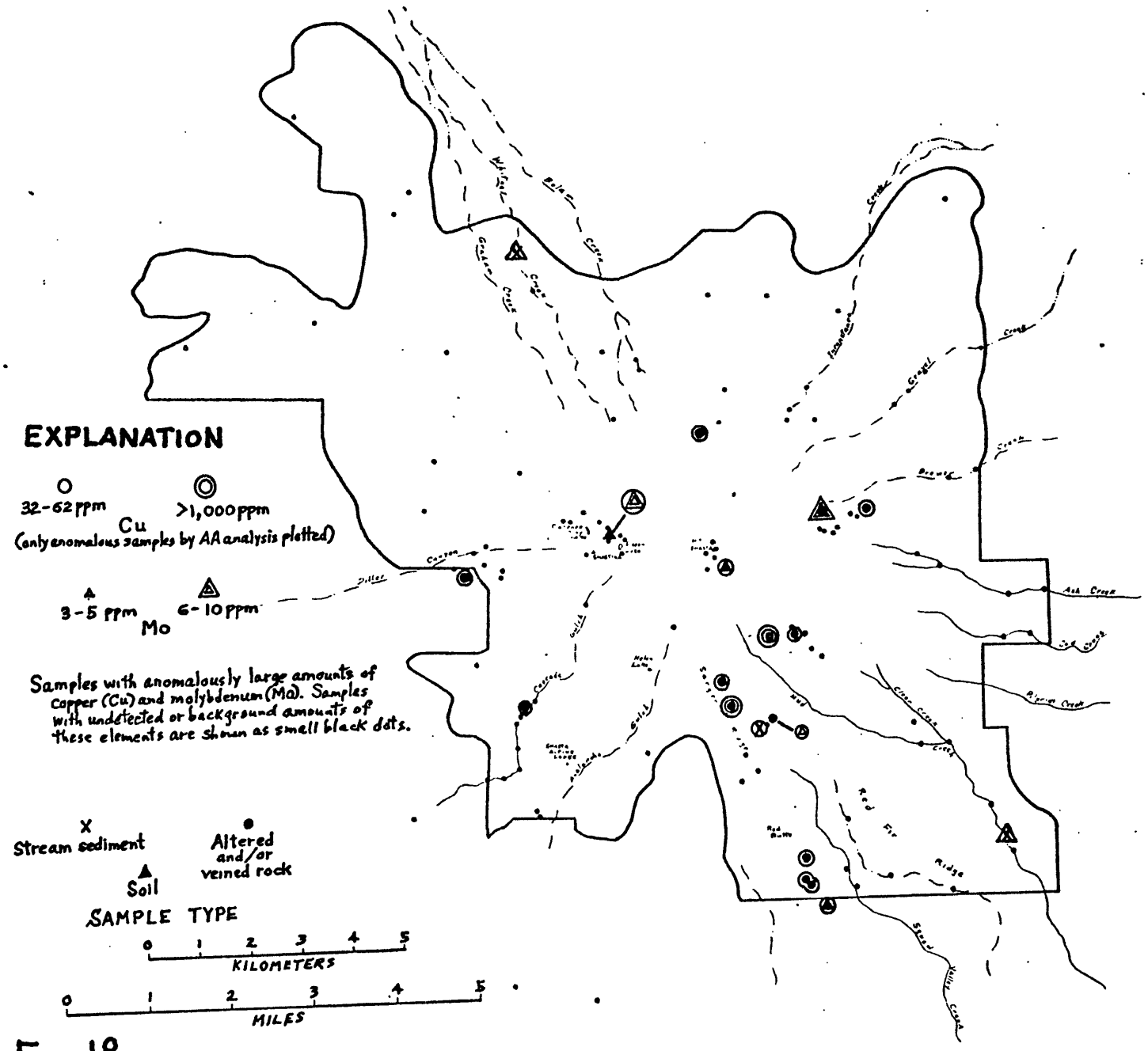
EXPLANATION
32-62 ppm
>1,000 ppm
Cu
(only anomalous samples by AA analysis plotted)
3-5 ppm
6-10 ppm
Mo
Samples with anomalously large amounts of copper (Cu) and molybdenum (Mo). Samples with undetected or background amounts of these elements are shown as small black dots.
Stream sediment
Altered and/or veined rock
Soil
SAMPLE TYPE
0 1 2 3 4 5
KILOMETERS
0 1 2 3 4 5
MILES
N

Fig. 18

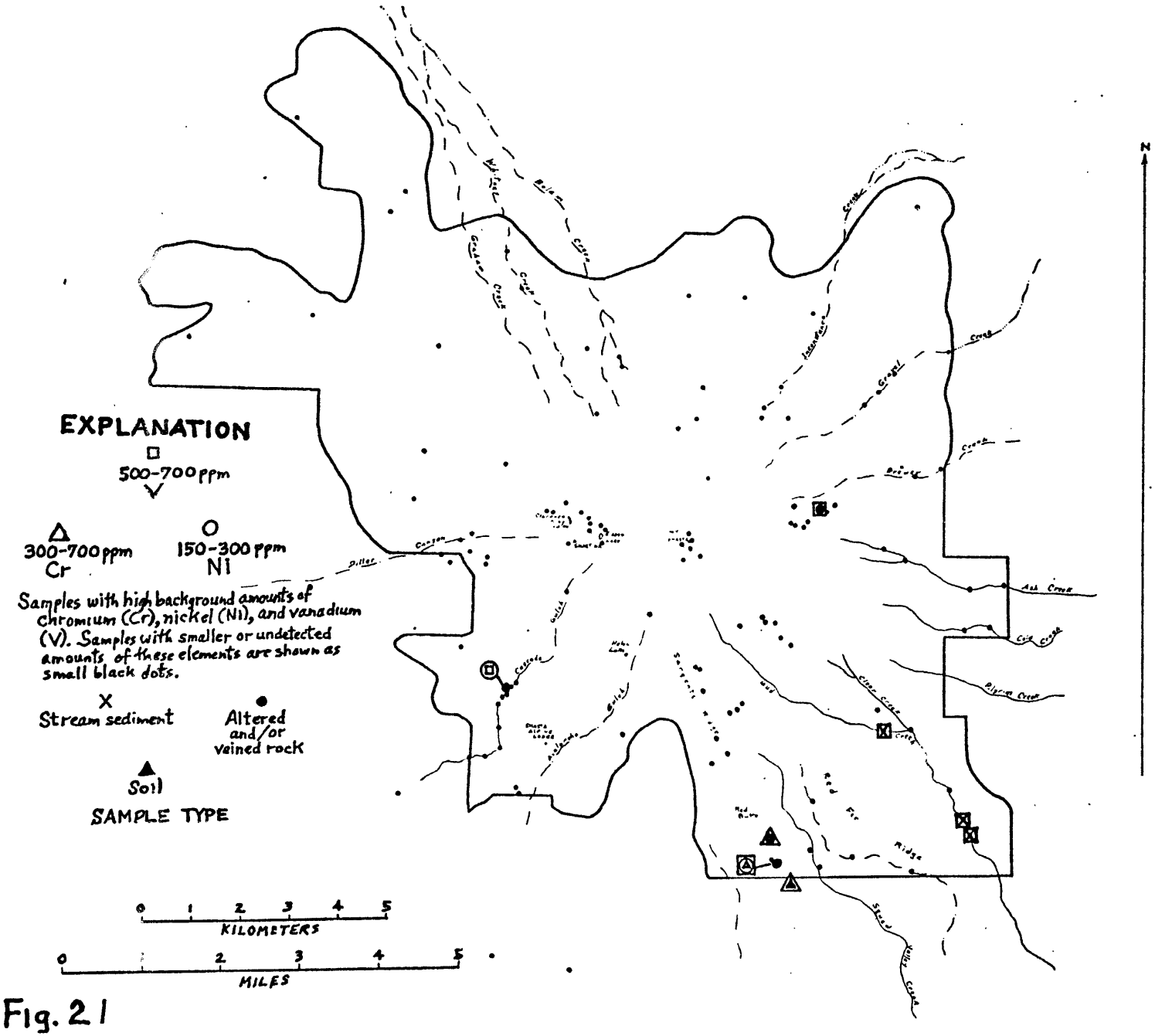
EXPLANATION
500-700 ppm
V
300-700 ppm
Cr
150-300 ppm
Ni
Samples with high background amounts of chromium (Cr), nickel (Ni), and vanadium (V). Samples with smaller or undetected amounts of these elements are shown as small black dots.
X
Stream sediment
Altered and/or veined rock
Soil
SAMPLE TYPE
0 1 2 3 4 5
KILOMETERS
0 2 3 4 5
MILES
N

Fig. 21

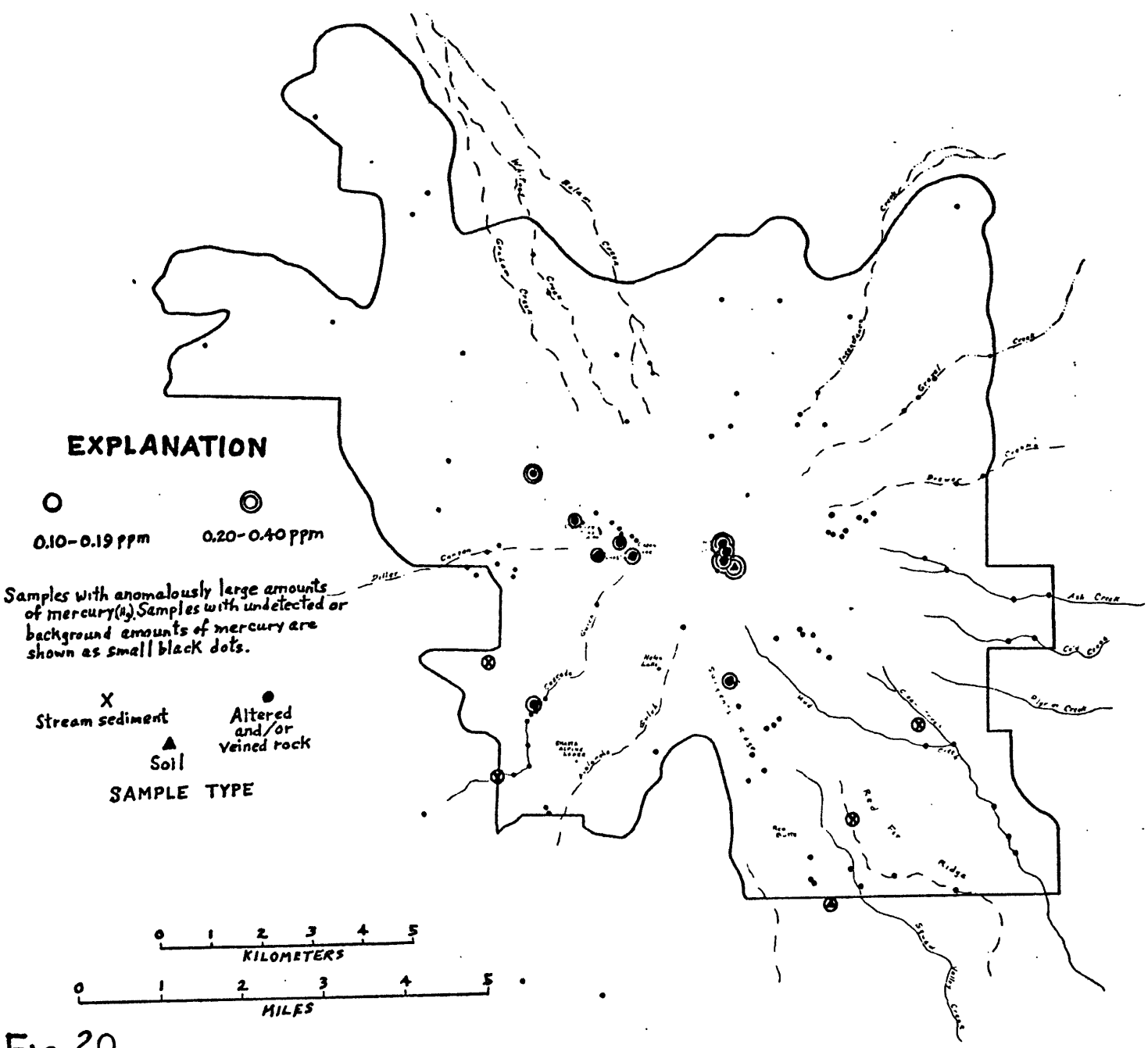
EXPLANATION
0.10–0.19 ppm
0.20–0.40 ppm
Samples with anomalously large amounts of mercury(Hg). Samples with undetected or background amounts of mercury are shown as small black dots.
X
Stream sediment
Altered and/or veined rock
Soil
SAMPLE TYPE
0 1 2 3 4 5
KILOMETERS
0 1 2 3 4 5
MILES
N

Fig. 20

FIG. 23

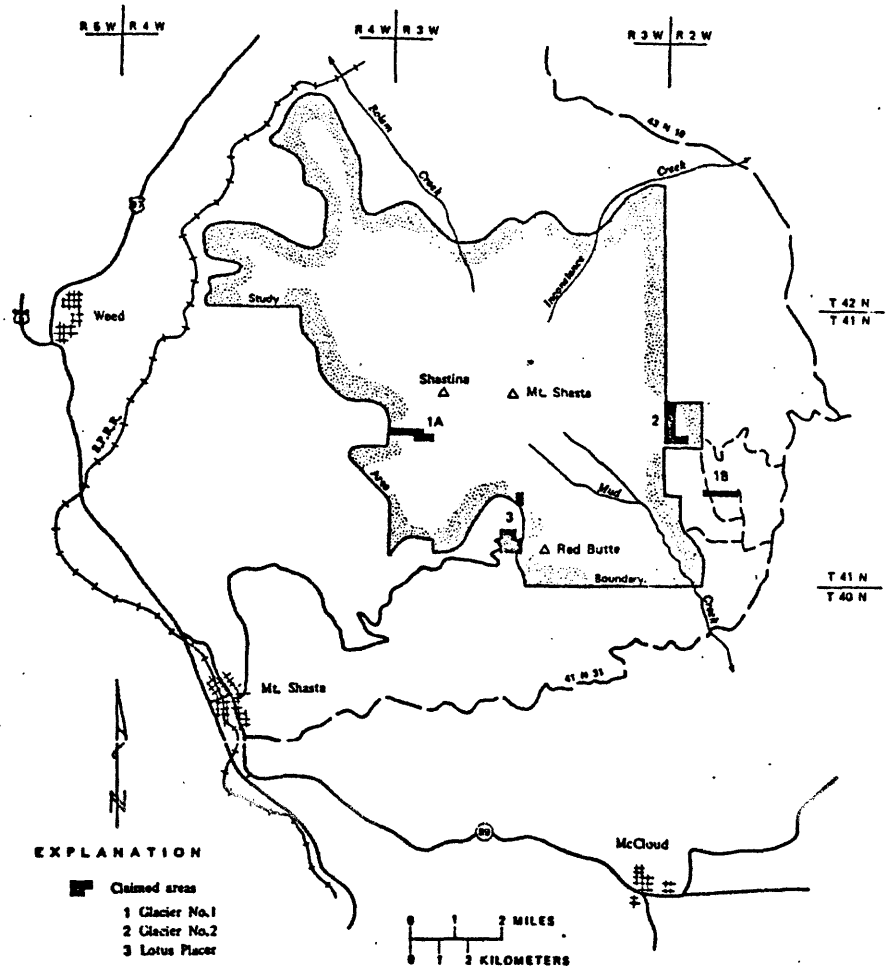
R 5 W
R 4 W
R 4 W
R 3 W
R 3 W
R 2 W
Weed
Study
Shastina
Mt. Shasta
Red Butte
Boundary
Mt. Shasta
McCloud
T 42 N
T 41 N
T 41 N
T 40 N
1A
2
1B
3
EXPLANATION
Claimed areas
1 Glacier No.1
2 Glacier No.2
3 Lotus Placer
0 1 2 MILES
0 1 2 KILOMETERS

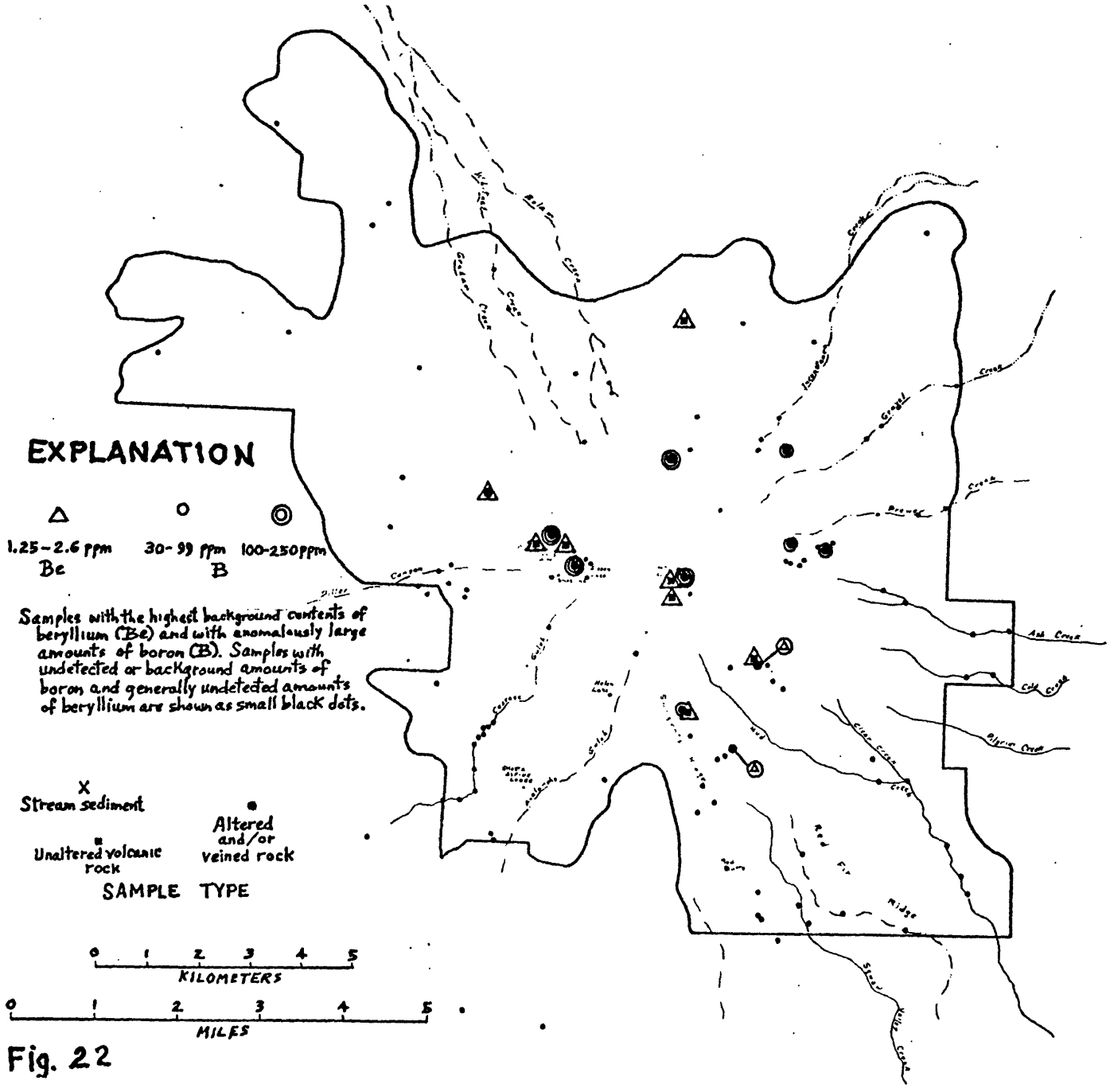
EXPLANATION
1.25–2.6 ppm Be
30–99 ppm B
100–250 ppm
Samples with the highest background contents of beryllium (Be) and with anomalously large amounts of boron (B). Samples with undetected or background amounts of boron and generally undetected amounts of beryllium are shown as small black dots.
Stream sediment
Unaltered volcanic rock
Altered and/or veined rock
SAMPLE TYPE
0 1 2 3 4 5
KILOMETERS
0 1 2 3 4 5
MILES
N

Fig. 22

Table 2.-- Chemical analyses of volcanic rocks of Mt. Shasta. New analyses by rapid-rock analysis methods (Shapiro, 1975), analyst H. Smith. Values in weight percent.

	1	2	3	4	5	6	7	8	9	10	11	12	13	14	15	16
Lithology	Basalt	Andesites								Dacites						
Location	Cinder cone	Avalanche Gulch	Clear Creek	Bolam Creek	Lava Park	Near Cinder Cone	Whitney Creek	McBride Springs	Northwest flank	South of Konwakiton Glacier	Misery Hill	Southwest of North Gate	North rim Shastina	South rim Shastina	Black Butte	Summit
Cone complex	Sargents Ridge	Misery Hill			Shastina					Sargents Ridge	Misery Hill		Shastina			Hotlum
SiO_2	52.03	61.0	62.3	63.6	61.17	61.20	62.74	62.74	63.0	63.6	63.7	64.2	63.6	63.6	65.67	64.9
Al_2O_3	16.51	17.3	16.9	16.5	16.58	16.53	16.54	16.53	16.8	16.7	18.0	17.5	17.1	17.5	17.52	16.7
Fe_2O_3	3.41	1.5	1.4	1.0	1.37	1.21	1.62	1.71	1.4	2.0	2.7	1.5	1.6	1.5	1.14	1.5
FeO	4.51	2.4	2.4	3.7	3.18	3.42	2.35	2.14	2.6	2.2	1.2	2.8	2.0	2.2	2.05	2.8
MgO	9.59	3.9	2.9	4.1	4.03	3.65	3.32	3.24	3.7	2.9	2.6	2.8	3.3	2.8	1.96	3.1
CaO	9.48	6.2	5.3	5.6	6.73	6.48	6.13	6.20	5.7	4.7	5.0	5.2	5.3	5.4	6.38	5.3
Na_2O	2.97	4.0	4.2	4.1	4.21	4.08	4.12	4.08	4.0	4.3	4.1	4.1	3.9	4.2	4.52	4.1
K_2O	.41	.78	1.4	1.4	1.05	1.16	1.20	1.18	1.2	1.9	1.3	1.5	.95	1.1	1.12	1.6
H_2O^+	.30	.29	.73	.47	.49	1.01	.67	1.02	.43	.89	.56	.50	.44	.55	.00	.34
H_2O^-	.09	.19	.14	.11	.14	.15	.26	.27	.18	.31	.41	.25	.48	.15	.03	.12
TiO_2	.66	.75	.60	.63	.69	.71	.58	.56	.60	.58	.62	.47	.49	.49	.42	.57
P_2O_5	.12	.17	.15	.14	.21	.24	.17	.16	.19	.14	.11	.14	.14	.12	.11	.13
MnO	.14	.06	.06	.07	.08	.08	.07	.07	.06	.06	.05	.06	.04	.05	.06	.07
CO_2		.01	.01	.01					.01	.02	.01	.02	.01	.01		.01
Sum	100.22	98.6	98.5	101.4	99.99	99.93	99.77	99.92	100.1	100.2	100.4	101.0	99.4	99.7	99.98	101.2
Data source	Smith and Carmichael (1968)	New (lab. no. W191392)	New (lab. no. W191383)	New (lab. no. W191377)	Smith and Carmichael (1968)	Smith and Carmichael (1968)	Smith and Carmichael (1968)	Smith and Carmichael (1968)	New (lab. no. W191378)	New (lab. no. W191374)	New (lab. no. W191376)	New (lab. no. W191373)	New (lab. no. W191380)	New (lab. no. W191381)	Smith and Carmichael (1968)	New (lab. no. W191375)

Table 1.--Major component cones of Mt. Shasta stratovolcano.

Major cone	Central vent	Principal flank vents	Estimated age limits (years)
Hotlum	Mt. Shasta summit	None	<4,500-190(?)
Shastina	Shastina summit	Black Butte	<12,000-9,400
Misery Hill	Misery Hill saddle	Southwest of North Gate, Gray Butte	<100,000-<12,000
Sargents Ridge	Head of Mud Creek	Red Butte, south of Gray Butte, McKenzie Butte, North Gate, northwest flank, Spring Hill	>100,000

Table 4.--Magnetic properties of samples from Mount Shasta. Symbols: J_R, natural remanent magnetization; X, susceptibility; Q, Koenigsberger ratio.

Sample	Volcanic cone	Rock type	$J_R \times 10^{-3}$ emu/cc	$X \times 10^{-3}$	Q
75SV-49	Sargents Ridge	Andesite	2.65	.988	5.1
75SH-283	Sargents Ridge	Andesite	.562	.726	1.5
75SH-195	Misery Hill	Andesite	.100	.652	.3
75SH-137A*	Misery Hill	Andesite	2.61	.765	6.5
75SV-24	Shastina	Andesite	.463	.747	1.2
75SH-236	Shastina	Andesite	2.78	.599	8.8
75SH-225	Shastina	Andesite	4.38	.873	9.5
75SH-209A	Shastina	Dacite/ pyroclastic	1.19	.694	3.2
75SH-306B*	Shastina	Dacite	1.40	.915	2.9
75SH-311*	Shastina	Dacite	5.00	.431	21.9
75SH-107	Hotlum	Andesite	1.30	1.23	2.0
75SH-179	Hotlum	Dacite	4.67	.379	23.3

*Demagnetizing experiments indicate that these samples have been affected by lightning strikes.

Table 3.--Inverse modeling results of aeromagnetic anomaly over Mt. Shasta. Symbols: J, intensity of magnetization; I, inclination; D, declination; R, correlation coefficient; S, normalized standard deviation.

Layers	J x 10^{-3} emu/cc	I	D	R	S
1 - 15	1.713	45.0	51.3	.93	.37
4 - 15	1.748	45.7	51.4	.92	.38
1 - 13	2.342	38.2	49.5	.88	.47
1 - 11	3.641	31.3	39.3	.77	.64
1 - 23	1.666	25.8	-14.3	.51	.86

Table 5.--Inverse modeling results of aeromagnetic anomaly over Ash Creek Butte. Symbols, same as table 3.

Layers	J x 10^{-3} emu/cc	I	D	R	S
7 - 8	2.973	31.3	23.0	.92	.39
5 - 8	1.663	31.4	21.6	.87	.48
1 - 8	1.331	33.2	23.7	.82	.57
1 - 7	1.349	35.8	23.1	.63	.77

[illegible]

Table 6 Trace element analyses of selected samples of rocks, stream sediments, and soils from Mt. Shasta Wilderness Study Area. Generally analyzed by semiquantitative emission spectrographic method; Au, As, Cu, Hg, Sb, and Zn determined by atomic absorption except where noted by asterisk. Fe, Mg, Ca, and Ti in percent; all other elements in ppm. Other symbols explained at bottom of table.

ANALYSIS SAMPLE NO.	Fe	Mg	Ca	Ti	Mn	Ag	As	Au	B	Ba	Be	Bi	Cd	Co	Cr	Cu	La	Mo	Nb	Ni	Pb	Pd	Pt	Sb	Sc	Sn	Sr	Te	U	V	W	Y	Zn	Zr	Hg	LABORATORY SAMPLE NO.
DM-004	5	3	5	.3	700	N	N*	N*	L20	300	N	N	N	20	100	30*	N	3	N	10	10	—	—	N*	15	N	1500	—	—	150	N	10	N*	100	.02	DM-004
-006	7(7)	3(5)	5(5)	.3(.5)	700(1,000)	N(N)	0.2	<.05	L20(L)	200(300)	N(N)	N(L)	N(N)	30(30)	150(150)	26	N(L)	5(5)	N(N)	10(10)	10(10)	—(—)	—(—)	0.3	15(20)	N(N)	1,500(1,000)	—(—)	—(—)	300(300)	N(N)	N(15)	85	70(100)	.02	-006
-009	3	3	3	.3	500	N	N*	N*	L20	300	N	N	N	15	100	30*	N	N	N	20	20	—	—	N*	10	N	1500	—	—	150	N	10	N*	70	.10	-009
-014	7(5)	3(5)	5(5)	.3(.5)	700(700)	N(N)	0.4	<.05	L20(N)	300(300)	N(N)	N(N)	N(N)	30(30)	70(70)	24	N(N)	3(N)	N(N)	70(50)	30(30)	—(—)	—(—)	.3	15(20)	N(N)	1,500(1,500)	—(—)	—(—)	150(200)	N(N)	15(10)	73	70(100)	.06	-014
-022	7	3	5	.3	700	N	0.4	<.05	L20	200	N	N	N	30	150	22	N	N	N	100	10	—	—	.2	30	N	1000	—	—	300	N	15	86	100	.01	-022
-027	7	3	5	.3	700	N	1.0	<.05	L20	300	N	N	N	20	100	24	N	N	N	70	15	—	—	<.1	15	N	1500	—	—	150	N	10	67	70	.10	-027
-029	7	5	7	.3	700	N	N*	N*	L20	300	N	N	N	30	150	28*	N	N	N	100	10	—	—	N*	20	N	1000	—	—	200	N	10	N*	70	.10	-029
-030	7(7)	3(5)	5(5)	.7(.7)	700(1,000)	N(N)	0.7	<.05	L20(N)	200(300)	N(N)	N(N)	N(N)	30(30)	150(150)	26	N(N)	3(N)	N(N)	100(70)	N(N)	—(—)	—(—)	<.1	20(20)	N(N)	1,500(1,500)	—(—)	—(—)	700(500)	N(N)	15(15)	92	150(70)	.08	-030
-031	7	3	5	.3	500	N	0.7	<.05	L20	300	N	N	N	30	150	28	N	N	N	70	10	—	—	<.1	15	N	1500	—	—	300	N	10	72	70	.05	-031
-033	10(10)	3(5)	5(5)	.3(.5)	700(1,000)	N(N)	0.7	<.05	L20(N)	200(300)	N(N)	N(N)	N(N)	30(30)	200(200)	26	N(N)	5(5)	N(N)	100(100)	N(10)	—(—)	—(—)	.1	20(30)	N(N)	1,500(1,500)	—(—)	—(—)	700(700)	N(N)	N(10)	115	70(100)	.04	-033
-043	5	3	5	.3	700	N	N*	N*	L20	300	N	N	N	15	100	50*	N	N	N	70	15	—	—	N*	15	N	1500	—	—	150	N	15	N*	100	.10	-043
-045	7(5)	3(3)	5(5)	.3(.5)	700(700)	N(N)	0.9	<.05	L20(N)	300(300)	N(N)	N(N)	N(N)	30(30)	200(150)	26	N(N)	N(N)	N(N)	100(70)	10(10)	—(—)	—(—)	<.1	20(20)	N(N)	700(1,000)	—(—)	—(—)	200(300)	N(N)	15(10)	73	100(100)	.04	-045
-047	7(7)	3(5)	5(5)	.3(.5)	700(700)	N(N)	1.0	<.05	L20(N)	300(300)	N(N)	N(N)	N(N)	30(30)	70(70)	40	N(N)	N(N)	N(N)	30(30)	N(N)	—(—)	—(—)	.2	15(15)	N(N)	700(1,000)	—(—)	—(—)	150(300)	N(N)	N(10)	93	150(70)	.30	-047
-048	7(5)	3(3)	7(3)	.3(.5)	700(500)	N(N)	2.4	<.05	L20(N)	150(100)	N(N)	N(N)	N(N)	20(15)	70(70)	38	N(N)	N(5)	N(N)	30(20)	150(150)	—(—)	—(—)	.9	N(5)	N(N)	1,000(500)	—(—)	—(—)	300(200)	N(N)	L20(N)	35	100(70)	.04	-048
-049	7(5)	3(5)	5(5)	.3(.5)	700(700)	N(N)	0.3	<.05	L20(N)	300(300)	1.5(1.5)	N(N)	N(N)	30(30)	200(150)	48	N(N)	N(N)	N(N)	150(100)	N(10)	—(—)	—(—)	.1	30(30)	N(N)	700(700)	—(—)	—(—)	200(300)	N(N)	20(N)	106	150(100)	.16	-049
-054	3	3	3	.3	300	N	0.7	<.05	300	150	N	N	N	15	70	16	N	N	N	50	15	—	—	.3	15	N	500	—	—	150	N	15	49	70	.01	-054
-055	7(5)	3(3)	5(5)	.3(.5)	500(500)	N(N)	0.4	<.05	100(70)	200(300)	1.5(1.5)	N(N)	N(N)	15(15)	150(100)	10	N(L)	N(L)	N(N)	70(50)	15(15)	—(—)	—(—)	4	15(20)	N(N)	700(700)	—(—)	—(—)	200(300)	N(N)	20(20)	48	100(150)	.06	-055
-056	3	1.5	2	.3	500	N	N*	N*	15	200	N	N	N	15	100	15*	N	N	N	30	N	—	—	N*	15	N	300	—	—	100	N	15	N*	70	.40	-056
-057	10(10)	2(1.5)	2(1)	.3	500(500)	N(N)	2.5	<.05	L20(N)	300(300)	1.5(1.5)	N(N)	N(N)	30(30)	100(100)	26	N(N)	N(N)	N(N)	50(30)	N(10)	—(—)	—(—)	.2	20(20)	N(N)	300(300)	—(—)	—(—)	200(150)	N(N)	20(20)	76	100(100)	.20	-057
-058	5(5)	3(3)	3(3)	.7(.7)	700(700)	N(N)	0.5	<.05	L20(N)	150(200)	N(N)	N(N)	N(N)	15(15)	70(100)	26	N(N)	N(N)	N(N)	70(50)	N(10)	—(—)	—(—)	.2	15(15)	20(20)	1000(1,000)	—(—)	—(—)	150(200)	N(N)	10(L)	49	70(100)	.04	-058
-060	7(5)	3(3)	7(5)	.3(.5)	700(500)	N(N)	7.1	<.05	70(50)	200(300)	N(N)	N(N)	N(N)	30(30)	70(100)	46	N(N)	N(5)	N(N)	70(50)	30(30)	—(—)	—(—)	.5	15(15)	N(N)	300(500)	—(—)	—(—)	150(200)	N(N)	N(N)	24	100(150)	.10	-060
-066	3(5)	3(3)	3(3)	.3(.5)	500(700)	N(N)	0.6	<.05	L20(N)	300(500)	N(L)	N(N)	N(N)	15(20)	100(100)	34	30(30)	N(N)	N(N)	70(70)	15(15)	—(—)	—(—)	.3	15(15)	N(N)	1,500(1,500)	—(—)	—(—)	150(200)	N(N)	15(15)	69	150(150)	.04	-066
-067	3(5)	3(5)	3(5)	.3(.5)	500(700)	N(N)	0.6	<.05	30(N)	300(300)	N(N)	N(N)	N(N)	20(15)	150(100)	36	20(N)	7(5)	N(N)	30(30)	15(15)	—(—)	—(—)	.3	N(10)	N(N)	1,500(1,500)	—(—)	—(—)	150(200)	N(N)	15(10)	53	150(100)	.04	-067
-069	5(5)	3(5)	5(5)	3(3)	700(700)	N(N)	0.4	<.05	N(N)	300(300)	N(N)	N(N)	N(N)	30(30)	100(100)	30	N(N)	N(N)	N(N)	30(30)	10(N)	—(—)	—(—)	.2	30(30)	N(N)	1,500(1,500)	—(—)	—(—)	300(300)	N(N)	10(10)	57	70(70)	.02	-069
-070	5(5)	3(5)	5(5)	3(3)	700(700)	N(N)	6.6	<.05	L20(N)	300(300)	N(N)	N(N)	N(N)	20(20)	70(70)	34	N(N)	N(N)	N(N)	70(50)	20(20)	—(—)	—(—)	.2	20(20)	N(N)	1,500(1,500)	—(—)	—(—)	300(300)	N(N)	N(N)	35	70(50)	.02	-070
-071	5(5)	3(5)	5(5)	.3(.5)	700(700)	N(N)	0.4	<.05	L20(N)	300(300)	N(N)	N(N)	N(N)	20(20)	50(50)	40	N(N)	N(N)	N(N)	100(70)	15(N)	—(—)	—(—)	.1	15(20)	N(N)	1,500(1,500)	—(—)	—(—)	150(150)	N(N)	N(N)	49	150(100)	.04	-071
-075	7(5)	3(5)	7(5)	.3(.5)	700(1,000)	N(N)	3.8	<.05	N(N)	300(300)	N(N)	N(N)	N(N)	7(5)	100(70)	28	N(N)	N(5)	N(N)	70(50)	15(N)	—(—)	—(—)	.1	20(20)	N(N)	1,500(1,500)	—(—)	—(—)	200(300)	N(N)	20(15)	85	300(200)	.02	-075
-076	7(5)	3(5)	5(5)	.3(.5)	700(700)	N(N)	1.2	<.05	20(20)	300(300)	N(N)	N(N)	N(N)	20(15)	70(70)	36	N(N)	N(N)	N(N)	70(50)	20(20)	—(—)	—(—)	.1	15(20)	N(N)	1,500(1,500)	—(—)	—(—)	200(300)	N(N)	15(10)	60	200(100)	.06	-076
-079	7(5)	3(3)	5(5)	.3(.5)	700(700)	N(N)	0.7	<.05	70(70)	200(300)	N(N)	N(N)	N(N)	20(15)	70(70)	30	N(N)	N(N)	N(N)	70(50)	15(10)	—(—)	—(—)	.2	15(20)	N(N)	1,500(1,500)	—(—)	—(—)	200(300)	N(N)	15(10)	87	200(150)	.04	-079
-080	7(5)	3(5)	5(5)	.3(.5)	700(700)	N(N)	6.1	<.05	30(30)	500(500)	1.5(1.5)	N(N)	N(N)	70(50)	50(70)	48	30(N)	N(N)	N(N)	70(50)	20(20)	—(—)	—(—)	.4	15(20)	N(N)	1,500(1,500)	—(—)	—(—)	300(300)	N(N)	20(15)	51	150(150)	.02	-080
-081	5(5)	3(5)	7(5)	.7(.5)	700(700)	N(N)	0.8	<.05	100(100)	300(300)	N(N)	N(N)	N(N)	15(5)	30(30)	30	N(N)	N(N)	N(N)	40(30)	20(20)	—(—)	—(—)	.2	10(15)	N(N)	500(500)	—(—)	—(—)	70(70)	N(N)	10(10)	32	200(150)	.06	-081
-083	3(5)	3(5)	3(5)	3(3)	500(500)	N(N)	2.1	<.05	150(150)	500(500)	N(N)	N(N)	N(N)	N(N)	30(30)	10	N(N)	N(N)	N(N)	100(70)	20(20)	—(—)	—(—)	.4	N(N)	N(N)	1,500(1,500)	—(—)	—(—)	150(150)	N(N)	15(10)	12	100(70)	.12	-083
-084	L5(5.0)	1(1)	L5(1)	.3(.5)	200(500)	N(N)	0.4	<.05	L20(N)	500(1,000)	N(N)	N(N)	N(N)	15(5)	30(30)	16	N(N)	N(N)	N(N)	L70(50)	L20(L0)	—(—)	—(—)	.3	30(30)	N(N)	1,500(1,500)	—(—)	—(—)	300(300)	N(N)	N(N)	20	150(100)	.35	-084
-086	L5(2.0)	L5(1.0)	.7(1.0)	.3(.5)	150(200)	N(N)	12.	<.05	70(70)	300(300)	N(N)	N(N)	N(N)	N(N)	30(30)	25	N(N)	N(N)	N(N)	N(N)	20(20)	N(N)	N(N)	.2	15(15)	N(N)	700(1,000)	—(—)	—(—)	200(300)	N(N)	N(N)	17	150(70)	.14	-086
-087	L5	.7	.7	.3	150	N	N*	N*	150	200	N	N	N	2	150	30*	N	N	N	15	L	—	—	N*	15	N	300	—	—	150	N	10	N*	100	.10	-087
-088	7(5)	3(10)	5(5)	3(2)	300(500)	N(N)	0.2	<.05	30(200)	300(300)	N(N)	N(N)	N(N)	N(N)	N(N)	10	N(N)	N(N)	N(N)	N(10)	5(N)	—(—)	—(—)	.2	N(N)	N(N)	500(500)	—(—)	—(—)	70(70)	N(N)	N(N)	8	150(70)	.12	-088
-090	L5(1.0)	3(5.0)	L5(.1)	.3(.5)	500(700)	N(N)	1.5	<.05	150(150)	150(150)	N(N)	N(N)	N(N)	5(L)	150(150)	20	N(N)	N(N)	N(N)	70(50)	L20(L0)	—(—)	—(—)	.1	5(N)	N(N)	500(500)	—(—)	—(—)	100(150)	N(N)	N(N)	15	70(70)	.02	-090
-091	3(5)	3(2)	5(5)	.3(.5)	700(500)	N(N)	0.9	<.05	L20(L)	300(300)	N(N)	N(N)	N(N)	15(15)	50(70)	22	N(N)	N(N)	N(N)	N(10)	30(30)	10(N)	—(—)	.3	15(15)	N(N)	1,500(1,500)	—(—)	—(—)	150(200)	N	15(L)	52	70(100)	.10	-091
-092	L5	.7	L5	.3	100	N	N*	N*	N	150	N	N	N	5	150	10*	N	N	N	30	L	—	—	N*	15	N	700	—	—	150	N	N	N*	70	.10	-092
-093	5(7)	3(5)	7(7)	.3(.5)	500(700)	N(N)	0.5	<.05	L20(N)	500(700)	N(N)	N(N)	N(N)	30(30)	150(200)	48	N(N)	N(N)	N(N)	30(20)	10(N)	—(—)	—(—)	.3	20(30)	N(N)	1,500(1,500)	—(—)	—(—)	300(300)	N(N)	15(10)	67	100(70)	.04	-093
-094	7(5)	3(5)	5(5)	.3(.5)	700(700)	N(N)	0.5	<.05	N(N)	300(500)	N(N)	N(N)	N(N)	20(20)	100(100)	62	N(N)	N(N)	N(N)	150(100)	10(N)	—(—)	—(—)	.3	15(20)	N(N)	1,500(2,000)	—(—)	—(—)	700(500)	N(N)	15(10)	62	150(100)	.10	-094
-096	3	3	3	.3	700	N	N*	N*	30	300	N	N	N	15	150	30*	N	10	N	50	10	—	—	N*	15	N	1500	—	—	300	N	15	N*	100	.01	-096
-100	5	3	3	.3	700	N	N*	N*	70	300	N	N	N	15	100	30*	N	N	N	70	10	—	—	N*	15	N	1500	—	—	150	N	15	N*	150	.02	-100
-103	5(5)	3(3)	5(5)	3(3)	700(700)	N(N)	0.5	<.05	15(N)	300(500)	N(N)	N(N)	N(N)	20(20)	30(30)	3500.	N(N)	N(N)	N(N)	50(50)	300(150)	—(—)	—(—)	.6	15(20)	N(N)	1,500(1,500)	—(—)	—(—)	300(300)	N(N)	15(10)	293	70(100)	.16	-103
-104	5(5)	3(5)	5(5)	3(3)	700(500)	N(N)	0.8	<.05	L20(N)	300(500)	N(N)	N(N)	N(N)	20(20)	20(20)	3870.	N(N)	N(N)	N(N)	50(50)	70(70)	—(—)	—(—)	.3	15(20)	N(N)	1,500(2,000)	—(—)	—(—)	300(300)	N(N)	15(10)	65	100(100)	.04	-104

L = Detected, but below limit of determination or below value shown
N = Not detected, at limit of detection
— = Not looked for
( ) = Second run

Table 8.--Zinc contents of selected samples. Analyzed by atomic-absorption method except values in parentheses by emission-spectrographic method. Values in ppm.

Laboratory sample no.	Sample Material			
	Unaltered volcanic rocks	Altered volcanic rocks or fracture coatings	Stream sediments	Soils
LDA-579	56			
LDA-581	63			
LDA-584	57	Average 59 range 56-63		
LDA-585	60			
LDA-586	59			
W-191374	(45.7)			
W-191375	(45.8)			
W-191376	(41.6)	Average 50		
W-191379	(64.8)	range 39-65		
W-191380	(39.3)			
W-191381	(61.0)			
W-191383	(33.9)			
Average of above 54.5 range 39-65				
LDA-054		49		
LDA-055		48		
LDA-057		76*		
LDA-058		49		
LDA-060		24		
LDA-065		70		
LDA-066		69		
LDA-067		53		
LDA-069		66		
LDA-070		35		
LDA-071		49		
LDA-075		85*		
LDA-076		60		
LDA-079		87*		
LDA-080		51		
LDA-081		32		
LDA-083		12		
LDA-084		20		
LDA-086		17		
LDA-088		8		
LDA-090		15		
LDA-091		52		
LDA-093		67		
LDA-094		62		
LDA-103		283*		
LDA-104		65		
		Average 57.5 range 8-283		
LCY-998			68	
LCY-999			63	
LDA-006			85*	
LDA-011			65	
LDA-013			65	
LDA-014			---	
LDA-022			86*	
LDA-024			57	
LDA-025			67	
LDA-030			92*	
LDA-031			72*	
LDA-033			115*	
LDA-035			49	
LDA-039			63	
LDA-045			73*	
			Average 33 range 49-115	
LDA-047				33
LDA-048				35
LDA-049				106*
LDA-050				60
LDA-051				65
				Average 60 range 33-106

* Marks anomalously large quantities of zinc for the area studied.

Table 7.--Averages and ranges of selected trace elements in unaltered volcanic rocks of Mt. Shasta. Analyzed by emission-spectrographic method, and where noted by*, by atomic-absorption method. <, less than limit of detectibility, as indicated. Values in ppm.

Element	Fourteen unaltered andesites		Seven unaltered dacites	
	Range	Average	Average	Range
B	<4.2-20	<4.2	25	12-35
Ba	200-300	286	450	230-690
Be	<0.7	<0.7	2	1.6-2.6
Bi	<5	<5	<4.6	<4.6
Co	15-20	15.4	12	11-13
Cr	30-100	71	78	34-150
Cu	7-30 (12-32)*	17.6 (21)*	19	5.6-28
La	<5	<5	<19	<15-25
Mo	<2	<2	<2.6	<2.2-4.8
Ni	30-70	67	41	19-80
Pb	<3.5-10	<3.5	8.7	5.2-13
Sb	<20	<20	<68	<68
Sc	15-20	15.4	14	13-15
Sn	<2	<2	<15	<15
Sr	1000-2000	1429	670	400-1000
V	150-200	175	113	100-130
Zn	(56-63)*	(59)*	50	39-65
Zr	70-150	89	200	110-250

Table 10.--Beryllium contents of samples with highest background quantities. Analyzed by emission-spectrographic method. Values in ppm.

Laboratory sample no.	Sample Material	
	Unaltered volcanic rocks	Altered volcanic rocks or fracture coatings
W191374	2.1	
W191375	1.8	
W191376	2.1	
W191379	2.4	
W191380	1.6	
W191381	1.8	
W191383	2.6	
LDA-057		1.5
LDA-067		1.25[1/]
LDA-080		1.25[1/]

[1/] Average of 2 analyses

Table 9.--Copper contents of selected samples. Analyses by atomic-absorption method except values in parentheses by emission-spectrographic method. Values in ppm.

Laboratory sample no.	Sample Material			
	Unaltered volcanic rocks	Altered volcanic rocks or fracture coatings	Stream sediments	Soils
W-191374	(24.8)			
W-191375	(17.4)			
W-191376	(5.59)			
W-191379	(23.7)			
W-191380	(10.2)			
W-191381	(23.3)			
W-191383	(28.4)			
	average 19			
LDA-579	12			
LDA-581	18			
LDA-584	32			
LDA-585	18			
LDA-586	26			
	average 21.2			
	Average of above 20.1 range 5.6-32			
LDA-054		16		
LDA-055		10		
LDA-057		26		
LDA-058		26		
LDA-060		(70) 46		
LDA-065		32		
LDA-066		34		
LDA-067		36		
LDA-069		(70) 50		
LDA-070		(95) 54		
LDA-071		(70) 40		
LDA-075		28		
LDA-076		(50) 36		
LDA-079		30		
LDA-080		(70) 48		
LDA-081		(85) 50		
LDA-083		10		
LDA-084		16		
LDA-086		(50) 26		
LDA-088		<10		
LDA-090		20		
LDA-091		26		
LDA-093		(70) 48		
LDA-094		(70) 62		
LDA-103		(5,000) 3500		
LDA-104		(6,200) 3870		
		Average 312; range <10-3780 Average, excluding -103 and -104, 31; range <10-62		
LCY-998			30	
LDY-999			28	
LDA-006			26	
LDA-011			28	
LDA-013			28	
LDA-014			34	
LDA-022			22	
LDA-024			30	
LDA-027			24	
LDA-030			26	
LDA-031			26	
LDA-033			26	
LDA-035			30	
LDA-039			32	
LDA-045			24	
			Average 27.6 Range 22-34	
LDA-047				(65) 40
LDA-048				(65) 38
LDA-049				(35) 48
LDA-050				24
LDA-051				26
				Average 35.2 Range 24-48

Table 11.--Boron contents of samples with values above background. Analyzed by emission spectrographic method. Values in ppm.

Laboratory sample no.	Sample Material
	Altered rocks or Fracture Coatings
LDA-054	250[1/]
LDA-055	85[1/]
LDA-060	60[1/]
LDA-067	30
LDA-079	70[1/]
LDA-081	150[1/]
LDA-083	150[1/]
LDA-086	70[1/]
LDA-088	250[1/]
LDA-090	150[1/]
LDA-096	30
LDA-100	70

[1/] Average of 2 analyses

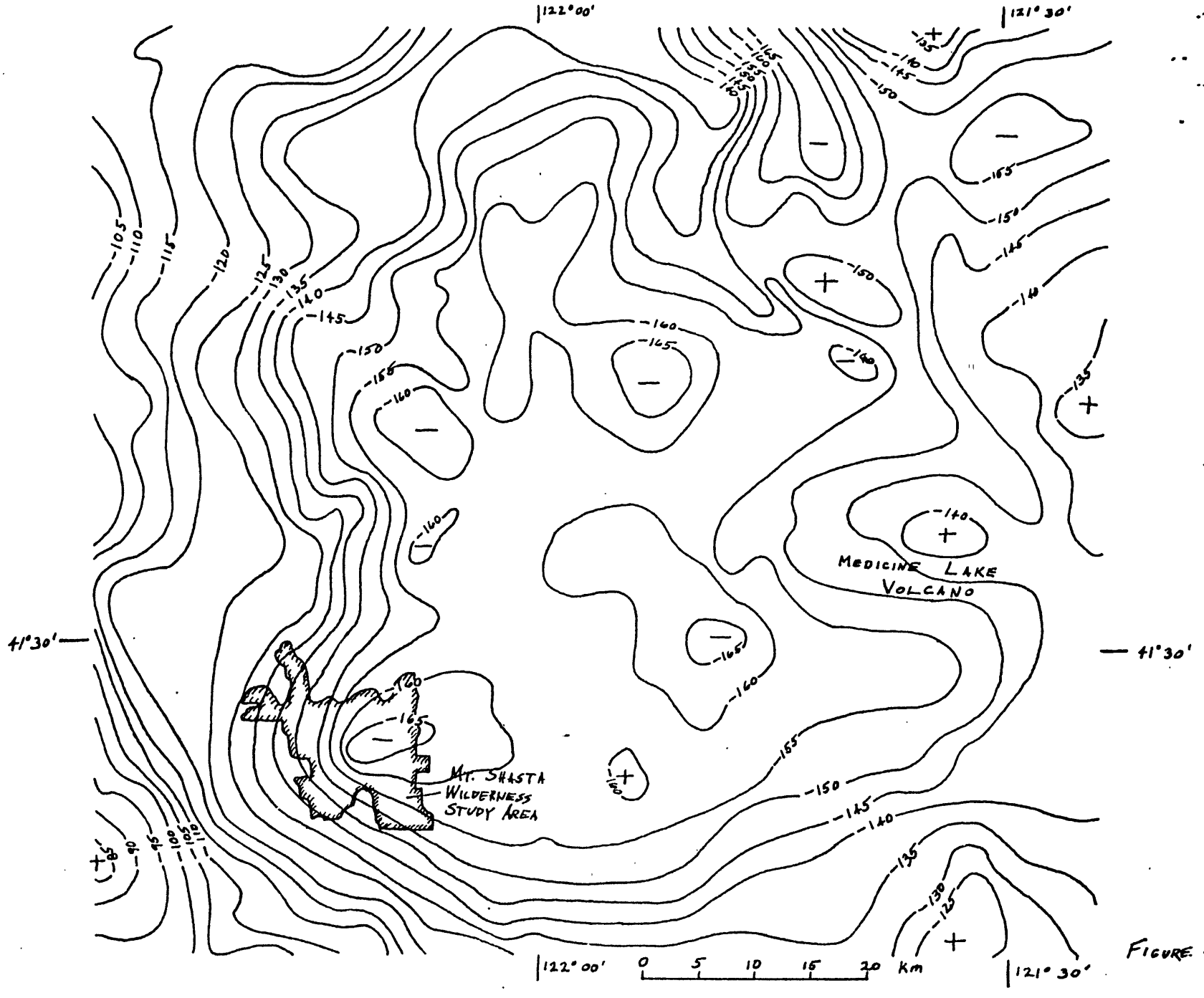
122°00'
121°30'
41°30'
MEDICINE LAKE VOLCANO
MT. SHASTA WILDERNESS STUDY AREA
0 5 10 15 20 km

FIGURE 4

FIGURE 5